Bachelor's Degree in Biomedical Engineering

Bachelor Thesis

DEVELOPMENT OF A HYPERSPECTRAL OPTICAL IMAGING SYSTEM

Author: Daniel García Alonso

Tutor: Yacine Babou

Co-tutor: Jorge Ripoll Lorenzo

AKNOWLEDGEMENTS

I would like to thank all the people that have made this project possible and have been by my side along all the path.

First of all I'd like to express my eternal gratitude to my supervisor Jorge Ripoll Lorenzo, who has teach me that the first step in solving a problem is leave out negativity, and has been extremely patient with me , as well as a huge help during the whole project.

In the same way, I would like to thank my tutor Yacine Babou, whose advices and leading along these last months has made this possible.

Thank you to all the teachers, in and out university, that with everyday effort they make possible that students can achieve their goals in life. We wouldn't be where we are without you all.

Thank you to all my friends, with whom I have shared my best and worst moments, but that are the best support when needed.

Special thanks to my family village, Coruña del Conde (Burgos), and all its people, that have shown me since the beginning that there are certain things money can't buy.

My most beloved gratitude goes to Blanca Zufiria, that has preventing me from giving up in the lowest moments, and didn't lose the faith on me when I had.

To all my family, brothers, grandparents, uncles… that have always support me in my decisions and have never let me down.

Finally, anything of these wouldn't be possible without my parents, that haven't left my side at any moment, and have always been proud of me. All my achievements are yours.

ABSTRACT

Motivation: the number of cancer cases at global level will increase from 12.7 million in 2008 to 21 million by 2030. Cancer treatment therefore represents a large clinical challenge that needs to be fulfilled.

Problem statement: There is an urgent need in the development of a system that allow to differentiate among healthy and cancer tissue in a fast accurate way. Hyperspectral imaging (HSI) techniques will be without doubt a main piece in the creation oncological diagnostic techniques.

Technical approach: The development of a HSI system in its first stages (no in-vivo nor in-vitro tests) that successfully acquire images in the hyperspectral domain. The use of galvo mirrors to scan a surface, in conjunction with a spectrometer that perform the light acquisition, with a LabVIEW program has been the first step.

Results: Performing the data analysis on a software like matlab has shown that the system works in a proper way, being the results satisfactory and as expected.

Conclusions: Further development will make possible to start working on in-vitro and in-vivo tests, and eventually in actual diagnostic techniques.

CONTENTS

LIST OF FIGURES

LIST OF TABLES

1. Introduction

Hyperspectral Imaging (HSI), also known also as Spectroscopic Imaging, is an emerging technique that integrates conventional imaging and spectroscopy to document on both spatial and spectral information of a given object. This technique generates very high-dimensional images through the use of sensor optics with a large number of nearly contiguous spectral bands. Due to this sampling strategy, hyperspectral images provide much more information about the captured scene than traditional solutions based on panchromatic or multispectral approaches.

In other term, this technique provides spatial (possibly spatiotemporal) distribution of the radiative or spectral signature associated to an object. And considering that the spectral signature is related to specific component, by combining the spectral information provided by spectroscopy and the spatial information provided by imaging, hyperspectral imaging (HSI) offers improved knowledge on the composition and distribution of components in an object. This technique HSI stands as reliant relevant and efficient approach. As a rule the technique is non-destructive, non-contact and can be faster than traditional techniques. Technological advances in spectrograph and detector design leading to decreased cost and improved instrumentation have enabled HSI applications to increase in number and widen in scope over the past twenty years.

There are many manufacturing processes that already take advantage of multi- or hyper-spectral data. These include processes such as inspection of colour and paint quality, detection of rust, or the inspection of defects in thin film coatings. HSI present a great potential for the on-line, real-time inspection/monitoring of the quality of various high temperature process, such as those involving welding. In this case the time evolution of spectroradiometric data can be translated to temperature maps and heat transfer processes in the welded parts. Heat flow maps can be correlated with good or cold welds. Real time detection of such defects can be used to correct the process before too

many defective parts leave the production line. The interest in food science and technology for HSI technique has considerably growth for various application [1] related to quality control of vegetable, fruit, grain, meat and poultry products.

In the medical field, hyperspectral imaging stands as emerging imaging modality for medical diagnosis and surgery and real-time systems are currently under development [2] for cancer surgery and diagnosis.

Based on data from the World Cancer Research Fund (WCRF International), the number of cancer cases at global level will increase from 12.7 million in 2008 to 21 million by 2030. Cancer treatment therefore represents a large clinical challenge which may be faced with HSI, considering its potential to differentiate healthy and diseased tissues and so lead to better surgical removal. To delineate remaining traces of malignant cells, the HSI can be used in an active mode in which the biological tissue is illuminated at wavelengths that causes the tissue to fluoresce. Typically this may include excitation in the UV or blue-green range of the spectrum and fluorescence measured at longer wavelengths. The fluorescence signatures of benign or malignant cells have been shown to sufficiently differ to allow discrimination [3] but the problem of detection of small signals embedded in a poor signal-to-noise and poor signal-to-background ratio remains.

The brain surgery is particularly delicate and requires more caution than for many other organs where the tumour removal with a surrounding rim of healthy tissue can be tolerated. HSI technique can be considerably beneficial for the procedure of brain tumours removal. There are several reasons for this. Brain tumours, more than any other cancers, can resemble the normal surrounding brain making them difficult to differentiate. Unlike many tumours, they infiltrate the surrounding tissue and thus their borders are indistinct and difficult to identify with standard imaging.

Currently the main tool for differentiating normal from malignant tissue remains the human eye. With the HSI, knowing the hyperspectral signatures of the healthy tissues and the same tissues affected by cancer, the degenerated tissue can be discriminated from the healthy one. Other techniques have been developed to enhance brain surgery (neuronavigation, ultrasound, Magnetic Resonance Imaging) but none has succeeded in reliable tissue differentiation. For instance MRI fails to provide real time images obtaining just an occasional snapshot during surgery. Under these circumstances,

hyperspectral imaging arises as a potential solution that allows a precise detection of the edges of the malignant tissues in real time, while assisting guidance for diagnosis during surgical interventions and treatment.

The potential of HSI is not limited to specific tissue identification and removal but concern the whole field of disease diagnosis and image-guided surgery. In addition to tumour delimitation and identification, medical applications of HSI concern, assessing tissue perfusion and its pathological conditions (including some complications like diabetic foot ulceration), making accurate surgical decisions, evaluating the health of dental structures, etc. Moreover, the cost associated with hyperspectral imaging instrumentation is significantly lower than the aforementioned techniques as it is based on conventional optical imaging technology. As a matter of fact, HSI technique supposes a non-contact, non-ionizing and minimal-invasive sensing approach based on registering extremely small wavelengths (normally in the nanometer range) of the tissues in order to determine their histological characteristics. It is clear that choosing the appropriate hyperspectral imaging system for each medical application, together with the most reliable hyperspectral image processing methods, are the main goals of future studies, before hyperspectral imaging becomes a widely applicable evaluation method in medicine.

From a deeper perspective the HSI will be a key tool to face health issues of the future. We understand health issue as any state in which it is required the attention of a medical expert, such as diseases causes by viruses, injures, cancer, obesity… And all the solving of these issues begins with an adequate diagnosis. In particular, the increase in the elderly population at the developed countries, and this percentage will be increased in the next decades, call for a better and faster healthcare attention. A stronger solicitation of the medical resources is expected, what will suppose a less effective medical response, for instance, in emergency situations.

In that emerging context, the development of better non-invasive diagnostic methods is necessary to reduce the medical interventions needed and hence the time spent by a doctor per patient. There is a need to develop easy reliable methods that speed up the processes in the resolution of health issues. A fast accurate and medical diagnosis can be capital in saving lives therefore there is a need to design and develop breakthrough

diagnostic approach that simplifies the resolution of problems related to heath issue increase. Ultimately a kind of diagnostics tool easy to operate as taking a picture. The HSI has the potential to achieve this goal.

With such tool, one can imagine that it will be even unnecessary for the patient to move to a hospital, since it can take some hyperspectral images by his own, and afterwards send it to the hospital. And even though it can only be used in medical centers, it is a fast procedure that will still saves load of time and lives.

But the objective of the work documented hereafter is more humble.

The intention of this thesis is to create a first-generation device that is able to obtain, analyze and display hyperspectral images, that afterwards can be kept developing to develop specific processing method for given applications. This work encompasses the development of an optical system, for hyperspectral imaging in the visible range. To ease the understanding, I will remind some fundamental information needed to afford the specifications related to hyperspectral imaging technique. The necessary background required for the Hyperspectral imaging technique is recalled in Section 2. The material used for the development of the setup is described in Sections 4 and 5. The assessment of the performances of the setup with simple case is reported in Section 6.

2. Background

The aim of the present section is to provide an outlook of the basic knowledge to tackle hyperspectral imaging technique requirements. In that frame, fundamentals on electromagnetic spectrum is first recalled. Then some specificities about the interaction of the light with biological tissues are sketched. The very basic aspects related to imaging technique and spectroscopy technique are briefly commented, in order to provide the key features of HSI technique arrangement and operation.

2.1. Visible light

The optical light, light accessible to human eye is an electromagnetic wave part of the electromagnetic spectrum. Electromagnetic spectrum refers to all possible wave of electromagnetic radiation. Electromagnetic monochromatic wave consists basically in the oscillations of electric and magnetic fields. Electromagnetic waves don't need a medium and can travel through vacuum (e.g. Light, X-rays, radio waves…) [4]

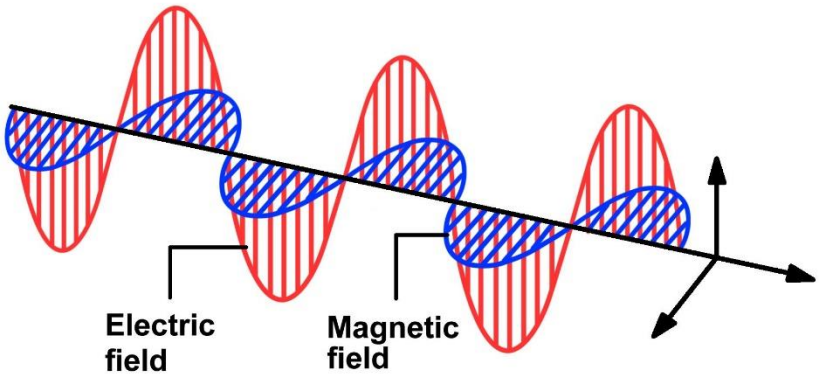

Figure 1. Representation of an electromagnetic wave [4]

Monochromatic waves are typically characterized by some quantity that are recalled.

- Period (T): Time the wave takes to go from a maximum peak to the next one.

Measured in seconds (s)

- Amplitude (A): Vertical distance from the mean value of the wave and the maximum one. Measured in metres
- Frequency (ν): Number of times a unit of the wave is repeated per unit of time. It is the inverse of the period.

  Its unit is the Hertz (Hz), what corresponds to s-1
- Wavelength (λ): It is the distance between the point and the same one in the next oscillation. Measured in meters.[5]

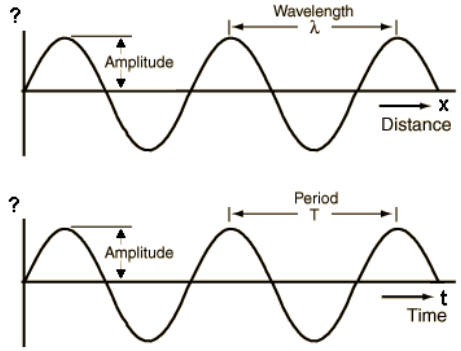

Figure 2 Representation of wave magnitudes [6]

From long wavelength radiation of radio waves to short wavelength gamma rays, there is a broad range of radiations, which each one has a different effect in the human body, as well in the rest of the matter. The longer the wavelength, the lower the energy of the radiation, and so the shorter the wavelength the higher the energy will be. Electromagnetic spectrum is usually represented as a wave whose wavelength increases. Human eye is able to recognize all the electromagnetic radiation with a wavelength between 400 and 700 and is called the visible domain of the electromagnetic spectrum. Above 700 nm, above the red colour we find infrared, whilst below 700 nm, below the purple, we find ultraviolet. Hence, red light is the least powerful. The behaviour of electromagnetic waves is described fully by the Maxwell equations, but there are not meaningful in the scope on this study and will not be presented.[7]

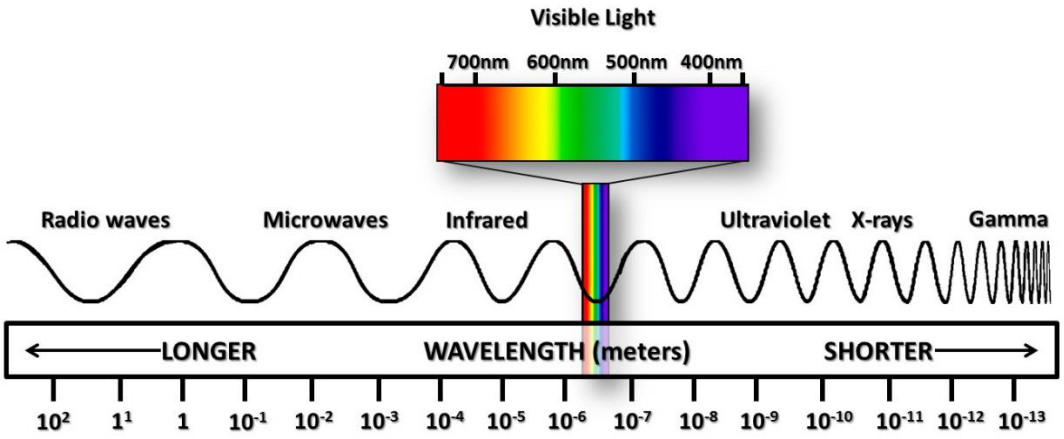

Figure 3. Electromagnetic spectrum with visible light range augmented [8]

2.2. Light-Biological tissue interaction

The interaction of the light with biological tissue is a must be clearly understood in order to develop reliable diagnostics based on optical imaging and or spectroscopic techniques. Although the present work does not deal with biological tissues, it sounds meaningful to incorporate some specificities of the biological tissue interaction with visible light. The characterisation of a biological tissue by means of optical diagnostics in the visible domain as to consider the fact that biological tissue do not emit light in the visible, while they emit thermal radiation. Hence, the light radiated by a biological tissue is always a light produce by a secondary source and transmitted by the tissue.

From a radiation point of view, biological tissues are highly heterogeneous medium that absorbs and scatters the visible light. As a rule in biomedical optics, light sources are placed on top of the tissue surface, either in contact or non-contact, and illuminate the tissue. The light interacting with a biological tissue will be subject to various processes that will affect its intensity and spectral distribution. These processes are schemed in Figure 4 [9].

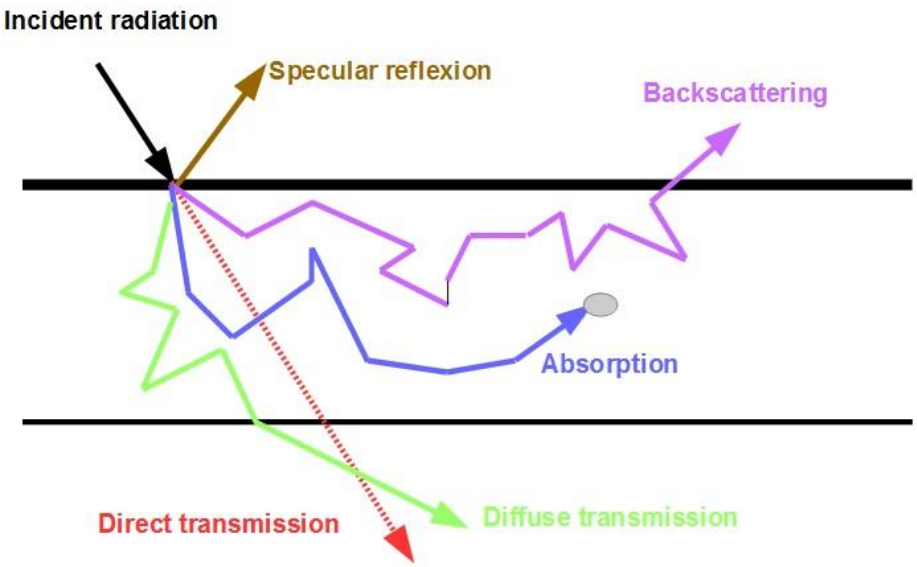

Figure 4. Main processes affecting the transport of the light in biological medium

A part of the incident light will be reflected by the surface and another part will be transmitted (direct or diffuse). The remaining part will undergo scattering by the tissue. The scattered photon can be either absorbed or radiated by the tissue toward a detector for diagnostic purpose. Depending on the structures constitutive of the tissue (e.g. cells) and their morphology, the tissue will manifest specific diffusion and absorption properties. Thus the transmission response (or backscattering) to an illumination (eg. by a short pulsed laser beam) is the signature of a well-defined tissue. Optical images of the reflected or trans-illuminated light are taken, which subsequently provide valuable biomedical information about macroscopic tissue changes.

Another radiative process can be used to probe a tissue, such as light fluorescence. Fluorescence may be produced by autofluorescence from the tissue chromophores. It can be also stimulated or induced by a laser. By illuminating a tissue with a laser of specific wavelength, the laser radiation at microscopic level interacts mainly with the outer electrons of the molecules. Upon absorption of a photon, a molecule is excited to a higher electronic state. This means that the molecule gains internal energy, but it is still intact with all electrons bound to the molecule. The excess energy absorbed in the molecule can, however, be transformed into heat or may cause chemical reactions which can damage the tissue. Besides, the molecule can also de-excite through the emission of a photon: this is the laser induced fluorescence that results in the emission of light from

the tissue with a specific spectral distribution.[10]

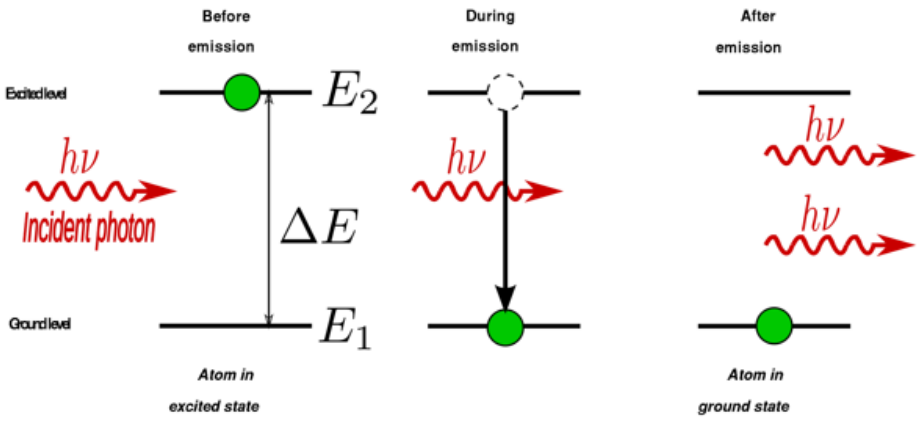

Figure 5. Stimulated emission principle [10]

The interaction of laser light with tissue is a well-suited selective tissue diagnostic tool since it involves the radiation of specific molecules within the tissues by means of laser excitation. This is due to the interaction between monochromatic light and several different molecules within the tissue, each molecule with its own spectrum. To understand the fluorescence spectrum from a certain kind of tissue, the mechanisms of interaction of both the excitation and fluorescence light with tissue are crucial, as is the fluorescence yields of the various chromophores.

Specifying the optical properties of a tissue is the first step toward properly designing devices, interpreting the measurements in a specific context.

2.3. Imaging techniques

The field of imaging technique especially in the bio medical field, is broad and it is not the pretention to introduce it here. However in the frame of this work some basic specificity is needed to be mentioned.

We will consider an imaging technique that is aimed to make an image, to record it thanks to an optical arrangement.

The simplest optical arrangement to make an image is to use a convergent thin lenses.

A lens is an optical device that is able to refract light beams. Shape of the lens will determine how it affects to light.

Lenses can focus light to form an image. That means that we can create an image of a sample (or anything whose light traverse the lens) on a certain plane by using lenses.

Lenses will focus light beams differently depending on their shape. The distance at which they focus light is known as focal length, and it is usually a known parameter of all lenses. This point where all light beams converges is known as focal point, and it is separated from the lens the focal length. [11]

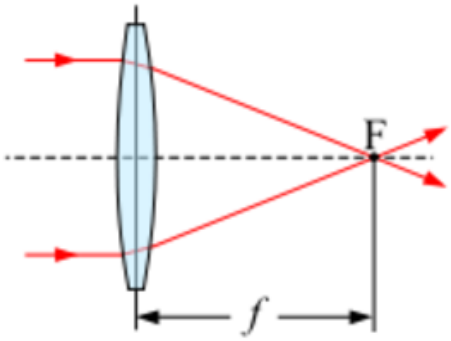

Figure 6. Focal distance and focal point of a biconvex lens as the ones used in this project. [11]

Nevertheless, the distance at which light beams are originated (i.e. where the sample is) will altered the distance at which they are focused.

This relation between the distance from the object to the lens, the distance at which the image is formed and the focal length of the lens is comprised in this equation. [12]

$$\frac{1}{S_1}+\frac{1}{S_2}=\frac{1}{f}$$

The distances correspond to the ones shown in this picture.

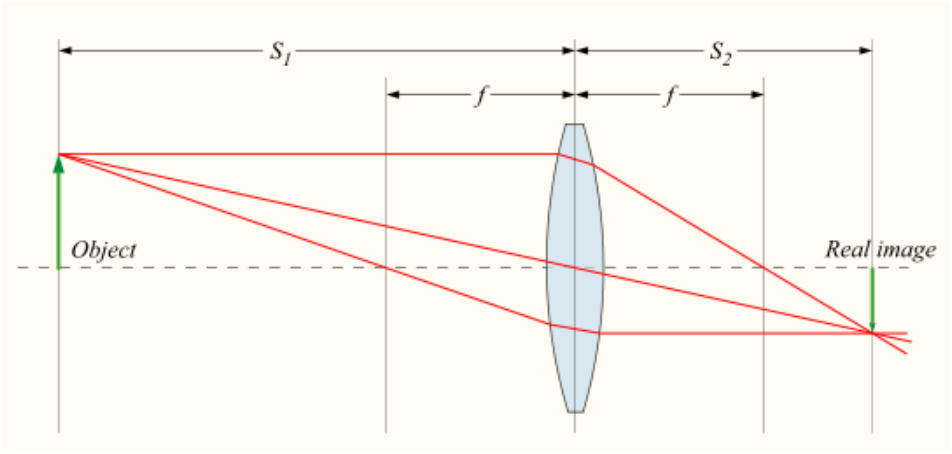

Figure 7. Image translation as a function of the focal length (f) and the distance between the object and the lens (S_1) [12]

2.4. Basics on Spectroscopy

Emission spectroscopy in the visible range is a spectroscopic technique which enable the analysis of the spectral distribution of the light by means of a spectroscope.
Visible light consists of electromagnetic radiation of different wavelengths in the range 400-700 nm. Not all emitted lights are perceptible to the naked eye, as the optical spectrum also includes ultraviolet rays and infrared lighting.[13]

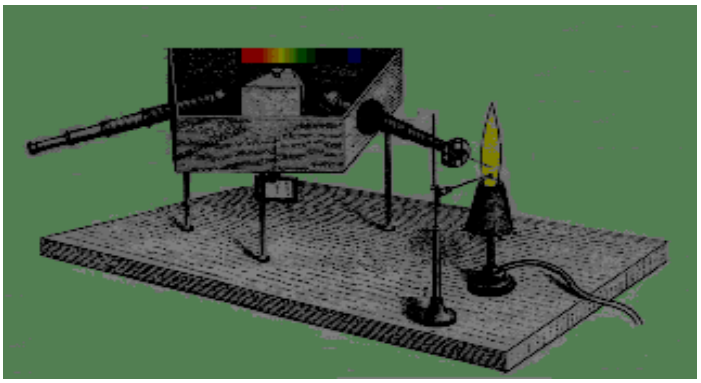

Figure 8. Drawing of the spectroscope developed by Bunsen et. G. R. Kirchoff. 1860

A spectroscope or a spectrometer is an instrument which is used for separating the components of light, which have different wavelengths. The spectrometer uses a dispersing element to produce the spectra of a light input. It has been developed initially by R. W. Bunsen et G. R .Kirchhoff for the application of element detection. They have shown that an element brought to high temperature emit light and the spectral distribution of this light is unique, it is a signature of the element. The example of a copper powder inserted into a flame is well known. By heating, the copper atoms are excited to high electronic levels. Then they emit a photon through the spontaneous emission process which bring the copper atoms to a lower energy level. The flame becomes green to the eye. The spectra associated to this green display a distribution of atomic emission lines. Each element emits a characteristic set of discrete wavelengths according to its electronic structure, and by observing these wavelengths the elemental composition of the sample can be determined. Emission spectroscopy developed in the

late 19th century and efforts in theoretical explanation of atomic emission spectra eventually led to quantum mechanics.

The typical arrangement of spectrometer is given in Figure 7. The incident light A enter in the spectrometer trough a slit and undergoes a first reflection by means of the primary mirror toward the dispersing element. At the time Bunsen and Kirchhoff, the dispersing element was a prism. Today as a rule the spectrometer uses a grating D. Then the light dispersed and reflected by the grating is reflected toward the secondary mirror E. The dispersed light is focalised onto the exit slit F that transmit the spectral distribution G of the initial incident light A.[14]

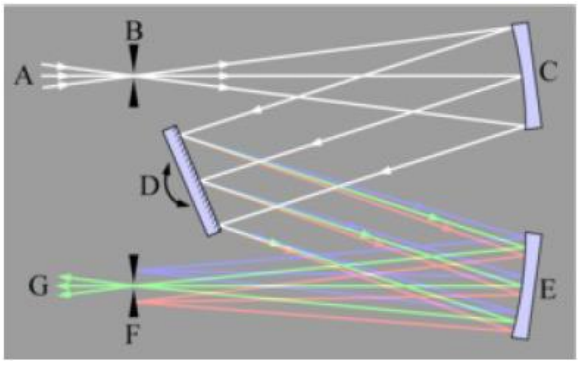

Figure 9. Scheme of the optical path in convention spectrometer

The spectral resolution is a key characteristic of the spectrometer and specify its capacity to separate monochromatic light. It is typically specified in nm and depends of the design and the performance of other items constitutive of the spectrometer. The spectral resolution limit is ruled by the dispersing element performance but also by the distance between the mirror and the dispersion component. As it can be identified on Figure XX, the longer is the distance between the grating D and the mirror E the broader is the separation between red, green and blue light.[15]

In current spectrometers, the detection of is performed by CCD technology. CCD devices are formed by 1D or 2D arrays of photodetectors. Photodetectors have the ability to transform a photon into an electrical charge. Although CCDs are not the only technology to allow light detection, it is widely used in medical and scientific applications. [16] Nowadays, small size spectrometer and even miniaturized spectrometer are available for a very moderate price and offering fair performances (spectral resolution of 1 nm).

To illustrate what is a spectrum in the visible, typical spectra acquired at 1nm spectral resolution, for a candle flame and a common light bulb are shown in Figure 8.

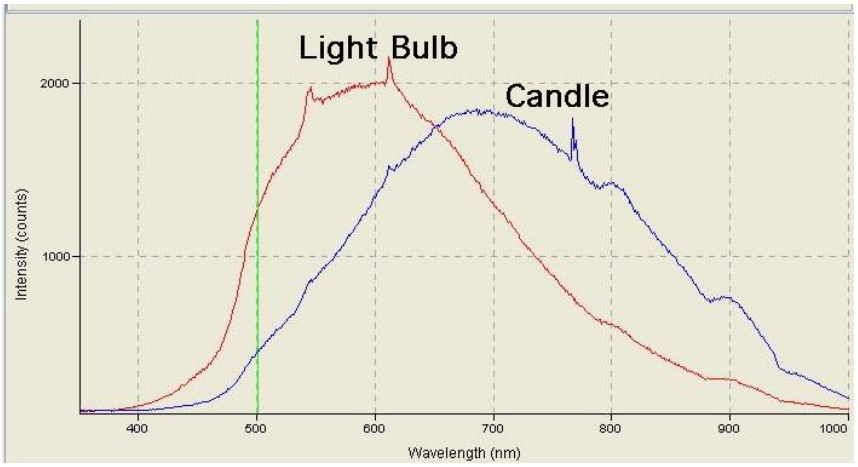

Figure 10. Typical spectra of light bulb and candle flame obtained in the visible and near infrared.[17]

2.5. Hyperspectral Imaging Technique

The HSI is by definition the combination of imaging and spectroscopy techniques. Hyperspectral imaging is part of a class of techniques commonly referred to as spectral imaging. Hyperspectral imaging is related to multispectral imaging. The distinction between hyper- and multi-spectral is sometimes based on an arbitrary "number of bands" or on the type of measurement, depending on what is appropriate to the purpose.

Multispectral systems obtain information in a few discrete spectral bands, while hyperspectral imaging systems acquire spectral data over a much broader spectral bands, as seen in figure XX. Hyperspectral deals with imaging narrow spectral bands over a continuous spectral range, and with the recording of the spectra of all pixels of the imaging frame. As a rule, images are obtained at sufficiently high spectral resolution to cover an extended continuous spectral domain.

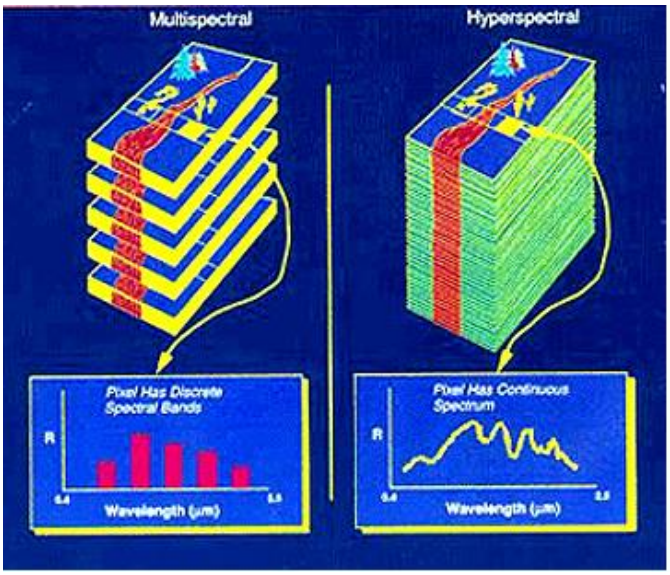

Figure 11. Comparison of multispectral and hyperspectral imaging [18]

In such manner, HSI provides a specific type of data: spatially and spectrally resolved information. HSI acquires a three-dimensional dataset often called hypercube, with two spatial dimensions and one spectral dimension. [18]

The arrangement adopted for HSI measurements therefore integrates the devices associated to imaging and spectroscopy techniques. Depending on the available devices different strategies can be used to capture hyper spectral images:

- Spatially Scanned Hyperspectral strategy. Where the spectral information is acquired without scanning in the spectral dimension. The spatial intensity over x, and y is instead obtained by scanning point-scanning, line-scanning.
- Spectrally Scanned Hyperspectral approach. Where the spatial information is recorded without scanning. The spectral information is instead obtained by scanning in the spectral domain. The light distribution I(x, y) is recorded for a specific monochromatic ('single-coloured') narrow spectral range. Then the scan is performed in spectral dimension to provide the hyperspectral data. Nowadays, commercial HSI devices for spectral scanning are typically based on optical band-pass filters (either tuneable or fixed). The scene is spectrally scanned by exchanging one filter after another.
- Snapshot Hyperspectral imaging system. In that case both the spectral and the

spatial information of a scene are simultaneously captured. Currently, this method provides low spatial or spectral resolution images. However, since all the information is captured in a single image, motion artefacts are eliminated. As a result, images can be captured at video rates, making this technology suitable for high speed applications.

Scanned Hyperspectral approaches can produce very high spatial and spectral resolution images. However, the time allocated for the scanning (spectral or spatial) is detrimental for achieving high temporal acquisition rate. As a result, any scanned system is inherently unsuitable for high speed applications. [19]

3. Project description

The aim of the project to design and build a hyperspectral optical imaging system. For this purpose, I have been working in the optical labs at Universidad Carlos III de Madrid, with the help and support of Jorge Ripoll and Yacine Babou. In the next part of the thesis I will explain the design of my device, both hardware and software, and the results I have obtained.

The system consists primarily in the coupling of a miniaturized spectrometer with galvo mirrors and additional optomechanical components to generate hyperspectral data.

The objective of this project is to pave the way towards the development of a highly versatile hyperspectral device for biomedical applications, but without limiting to this field. More specifically, the thesis objectives can be defined as:

- Development of a complex optical equipment in which several devices work simultaneously in an appropriate manner so the data obtained are accurate and reliable. The devices will be controlled with LabVIEW software.
- The assessment of a calibration method in order to apply the technique in various contexts.
- Implement a robust program suited to process and analyse the hypercube data. The software used for this step is a program developed in Matlab.

The analysis step can have different goals, depending on what it is characterized and hence what information is needed to be displayed.

During the whole process I have had to face several problems for whom I found an adequate solution in each case.

4. Materials and Methods

4.1. System Assembly

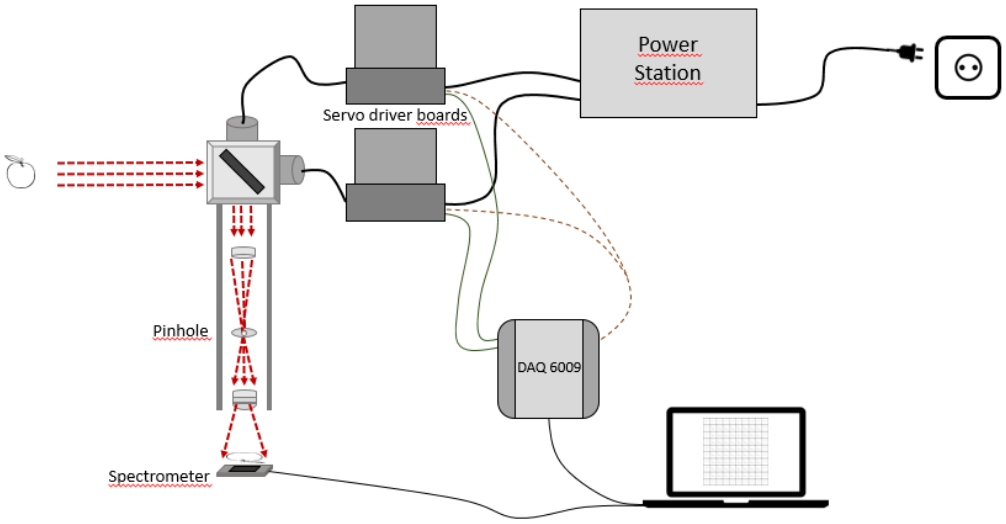

Figure 12. Scheme of the device.

The main task during the development of the device itself, independently on the analysis process or the simple used in the measurements was the correct synchronization of the galvo mirrors and the spectrometer.

The proper way of this to function is:

1. The galvo mirrors moves to the first position.
2. The spectrometer measures the spectrum of that point
3. Once the spectrometer finishes measuring the spectrum and not before, the galvo mirrors move to the next position
4. Spectrometer measures the new spectrum.
5. Repeat the process until all points have been scanned.

In the upcoming sections I am going to explain the main parts of the project, how they work and the use I have given them.

4.1.1. Galvanometer mirrors

2-Axis component in which each axis comprises a mirror, a motor assembly and a servo driver board.

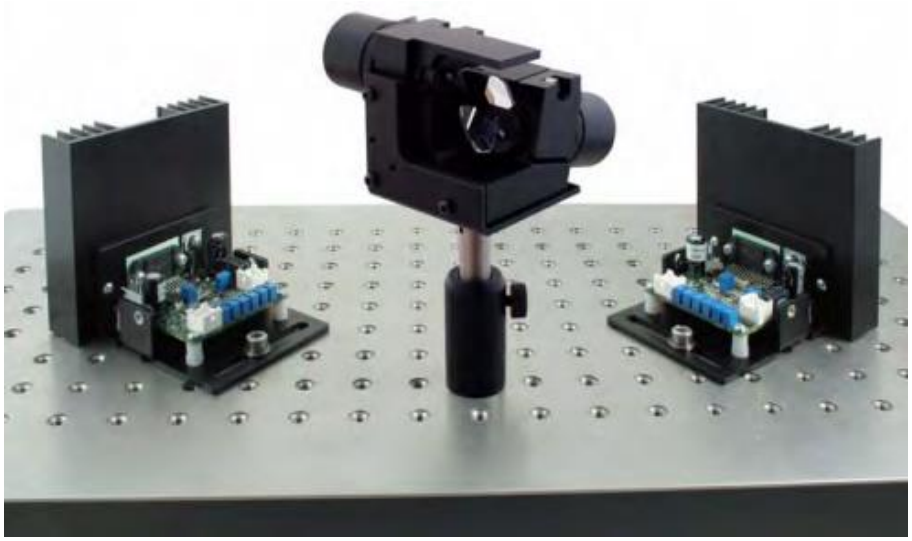

Figure 13. GVS012 2-Axis Thorlabs Galvo system [20]

A galvanometer is a precision motor with a travel of much less than 360º, whose movement is directly proportional to the current applied to the motor. When current is applied, the motor rotates through an arc, and it stops when applying a current of reverse polarity. If the current is removed the motor comes to rest. It consists of two main components:

- A motor that moves the mirror
- A detector that sends back information of the position of the mirror to the information system

All this means that by applying a certain current within a range, the motor will move the mirror a specific angle.

The mirror is attached to the end of the motor actuator, and it deflects the light over the angular range of the motor shaft.

The servo driver board is composed of a circuit that interprets the signals to drive the actuator to the demanded position. [20]

Each motor receives an independent current with a range of ±5V. Moreover, in the servo driver board the ratio V/º can be chosen. 1V/º, 0.8V/º and 0.5V/º are the three options you can work with. In this project I have used the latter one, in order to have a better resolution. Regarding these specification, we can calculate that the angle range at which the mirrors are able to move is ±10º.

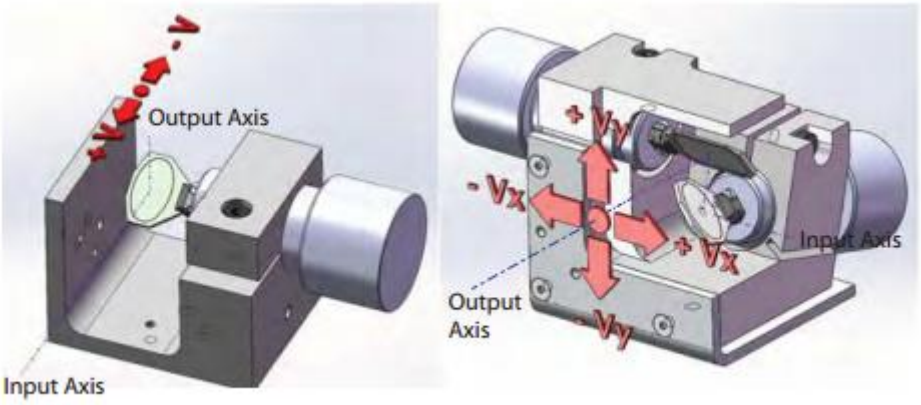

Figure 14. Single and dual axis voltage-dependent mirror movement [20]

Moreover, knowing the scanning angle and the distance of the sample to be scanned, scanning area can be easily calculated, as shown in figure XX.

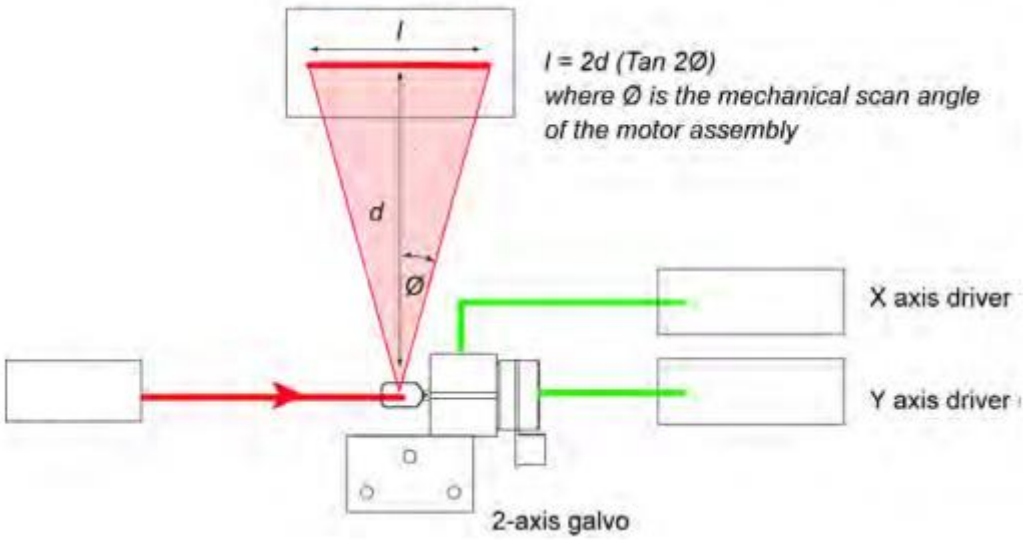

Figure 15. Scanning area as a function of distance and maximum angle. [20]

4.1.2. NI USB DAQ-6009

DAQ-6009 is the device used to convert the digital signal coming from the computer into an analog signal necessary for the galvanometer to work. It works as the bridge between the digital and analog fields of the project. The software used to control DAQ assistant is NI LabVIEW, compatible with both the DAQ and the spectrometer.

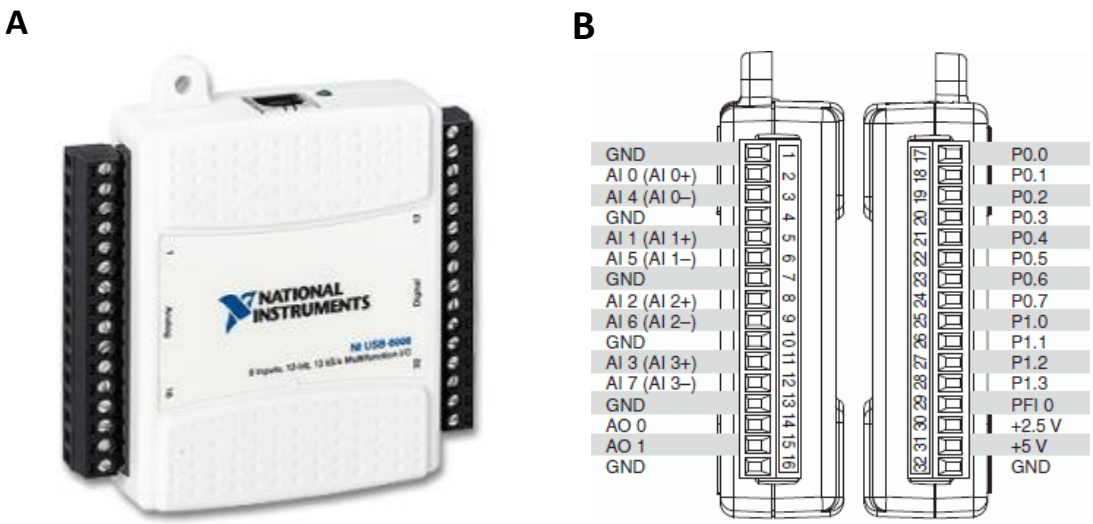

Figure 16. A: NI DAQ USB-6009. B: Signal labels [21]

I have been working with pins 14, 15, and 30. AO 0 and AO 1 are channels that supplies voltage outputs. Each one is connected to a mirror of the galvanometer. +2.5V channel is an output that stablish the current range accepted to work with. Hence, the range current at which the DAQ works is ±2.5V. It has been previously stated that galvanometer works in a range of 10V, but the DAQ makes a restriction for current values >5V. Hence, our galvo mirrors will work in the range of ±2.5V, reducing as well the angle range to ±5º. [21]

4.1.3. Lenses

The lenses used had a focal length of f=40 mm and f=30mm. This means that their focal point will be 4 and 3 cm respectively from the lens. Nevertheless, the image is not formed in the focal point.

A B

Figure 17. Thorlabs lenses used in the Project. A: f=40mm. B: f=30mm.

The other type of lens used was a cylindrical lens. The main different between these previous lenses and a cylindrical one is that it focuses light beams in a line instead of a point. [22]

Figure 18. Cylindrical lens with a focal length of f=50mm.

4.1.4. Pinhole

A pinhole was placed at the distance in which the image was formed after the first lens. This way, we would get rid of most of the image, only keeping a small point, which is the one whose light is measured. Leaving all the image to get to the spectrometer would suppose in inaccurate spectra. This subject will be better explained in the assembly section.

Figure 19. Thorlabs diaphragm used as pinhole

4.1.5. Spectrometer

The spectrometer is the most important part of the device. It is the one used to make the measurements of the spectra.

Figure 20. Light path in spectroscopy technique

The spectrometer used was bought to Ocean Optics and it is a model SPARK-VIS. It is a small light spectrometer that works in the spectral range that goes from 380nm to 700nm in wavelength, so it corresponds to the visible light range. Its size and ease of usage were the main reasons that determined that this would be the spectrometer used in the project, but it can be easily replaced with any other device.

Figure 21. Ocean Optics' spectrometer SPARK-VIS [23]

The spectrometer is directly connected to the computer via USB, and it was controlled by a LabVIEW software.

Specification	Spark-VIS	Spark-OEM-VIS	Spark-DET-VIS
Spectroscopic			
Spectral Range	380 to 700 nm		
Optical resolution	4.5 to 9.0 nm FWHM (~1.2% wavelength)		
Signal-to-noise ratio	1500:1		
Electronic			
A/D resolution	14 bit	N/A	
Power consumption	250 mA @ 5 VDC	30 mA @ 5 VDC	
Connector	micro-B USB (power and signal)	12-pin (0.5 mm pitch) ribbon cable	14-pin (7 x 2) connector
Detector			
Detector	Panavision ELIS1024 linear silicon CMOS array		
Integration time	10 µs to 10 s		
Pixels	1024		
Physical			
Operating temperature	-10 to 60 °C		
Relative humidity	0 to 85 % (non-condensing)		
Dimensions (L x W x H)	53.3 x 36.4 x 19.9 mm	38.4 x 22.6 x 10.2 mm	18.42 x 9.65 x 9.53 mm
Weight	15 g	3.8 g	<1 g

Table 1. Ocean Optics SPARK-VIS specifications [23]

The light is captured through a 1x8mm slit, where the sensor is placed. The detector assembled within this spectrometer a “Panavision ELIS 1024 linear silicon CMOS array”. The optical resolution of the device itself is pretty weak (~ 5-10 nm). The whole slit extension must be illuminated in order to assure that all the detector pixels receive light. This was a major issue that lead to some problems that needed to be solved afterwards. It will be explained in the assembly section.

4.2. Spectral intensity calibration procedure

The calibration is an essential step in all optical spectroscopy technique. Although it may seems that the spectrum acquired is an appropriate result, there are a lot of surrounding factors that can affect the measurements, for instance light of the surroundings, vibrations of the device… Above all, the calibration is necessary to inform about the spectral transmission along the whole optical system (that includes, lenses, mirrors, spectrometer detector…). Performing a calibration is necessary to correct from all these effects.

In order to achieve that, a calibration source with its documented spectral irradiance $S_{\lambda}^{cal\_lamp}$ is needed.

In this work, the calibration has been performed with an ocean optics DH-2000 deuterium-halogen light source.

Figure 22. Ocean optics DH-2000 calibration lamp [24]

This lamp have two type of light source; halogen, and deuterium. I have used the halogen one, since it is calibrated for the visible range, while deuterium is thought to be used in UV range. [24]

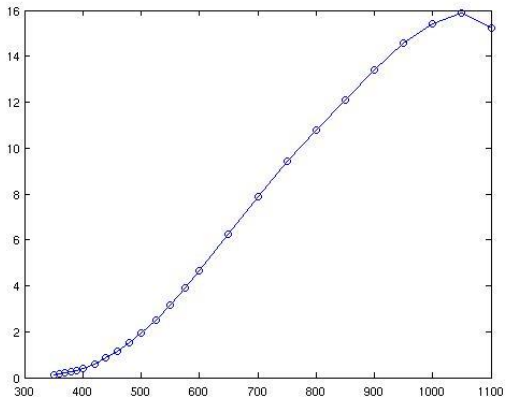

Figure 23. $S_\lambda^{cal\_lamp}$. Halogen light spectrum provided by Ocean Optics

After measuring the spectrum of the lamp, and having as well the data of the theoretical spectrum $S_\lambda^{cal\_lamp}$, the spectral response of the optical system can be determined. It is required that the halogen light measurement must be taken in the exact same conditions as the experiment is performed. Afterwards, this correlation must be applied:

$$S_\lambda^{cal} = S_\lambda^{corr} \times \left(\frac{S_\lambda^{cal\_lamp}}{S_\lambda^{meas\_lamp}}\right)$$

Where S_λ^{corr} is calculated as:

$$S_\lambda^{corr} = S_\lambda^{meas} - S_\lambda^{bg}$$

S_λ^{meas} is the spectrum of the studied sample measured by the spectrometer, S_λ^{bg} is the spectrum of the background of the environment when the experiment is performed. This spectrum is acquired by removing the studied sample. In other words it acquires all reminiscent light coming from surroundings except the sample itself. The spectrum recorded will look noisy because of the dark current. By subtracting this latter spectrum to S_λ^{meas}, we obtain a corrected spectrum, S_λ^{corr}, where background information has been removed.

After having performed the correction step, the calibration must take place. $S_\lambda^{meas\_lamp}$ corresponds to the spectrum recorded by the spectrometer of the halogen lamp light in the same conditions as S_λ^{meas} are taken.

S is indexed in λ, since it is a spectral distribution of the light intensity.

This calibration procedure is performed in the Matlab development section, and the development of this process is explained in that section.

4.3. Assembly

The correct assembly and arrangement of all the devices and materials is the most demanding part of the whole project. I had to face several obstacles that required to change the approaches to create an effective hyperspectral imaging device.

First of all, I want to talk about the sample used for the measurements. As a first approach, I used my own mobile phone that offers a broad choice of images to characterize, including black and white, colour images with high contrast, images with well-defined shapes… Moreover, since it is a screen. Nevertheless, this wouldn't have any practical application, since the device it is intended to be used with real samples. Still, it has shown to be a relevant first approach of the subject.

The first try was based in the use of a single lens.

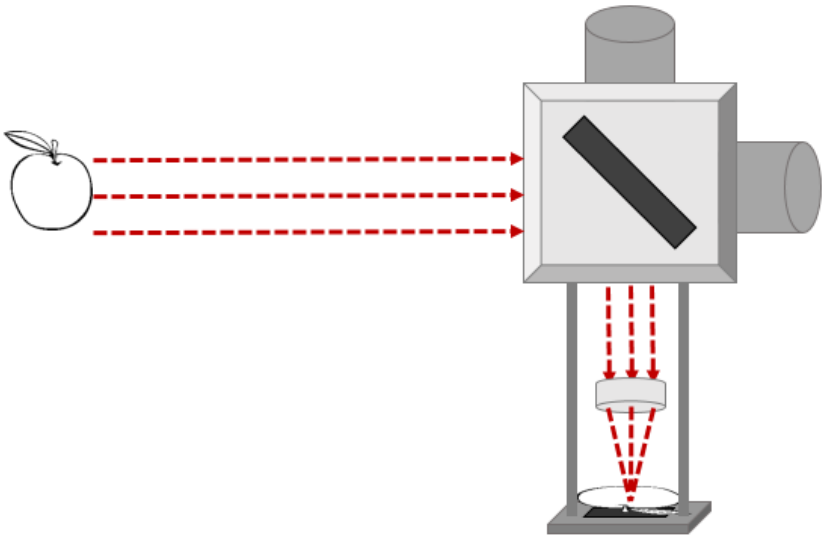

Figure 24. First arrangement of the device with a single lens.

The lens is used to image the studied sample on a plane of well-defined location, exactly where the spectrometer is placed. In order to find where to place the lens and the spectrometer it was necessary to know the distance between the mobile phone and the galvo mirrors, and the focal length f of the lens. In a first moment, I randomly placed the mobile at 23cm from the galvos, and so I established that distance as the standard point at which the mobile phone should be placed for future tests.

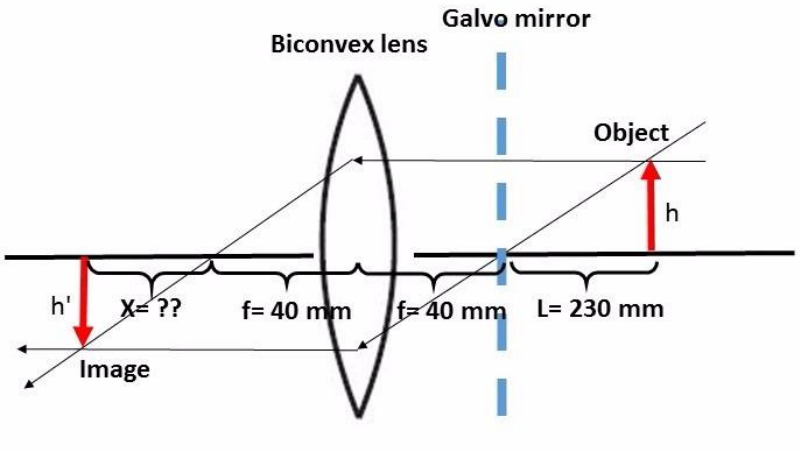

Figure 25. Arrangement of the lens.

The calculations performed to find that distance at which the image is formed, and hence where the spectrometer must be placed are the following, using the equation of the lenses stated in the lenses section.

$$\frac{1}{230+40}+\frac{1}{x+40}=\frac{1}{40}$$

After solving it for the value of x, we obtain that x=69mm. Hence the distance, at which the spectrometer should be placed is$\sim 47mm$.

The first attempts to obtain a focused image were performed with this configuration, but the ones obtained were nothing but a lot of pixels with apparent random values. After several attempts without success I realized that the image formed in the plane of the spectrometer was covered almost entirely by its slit. This resulted that it was obtained a lot of information of a wide area of the object, not of a small point of it.

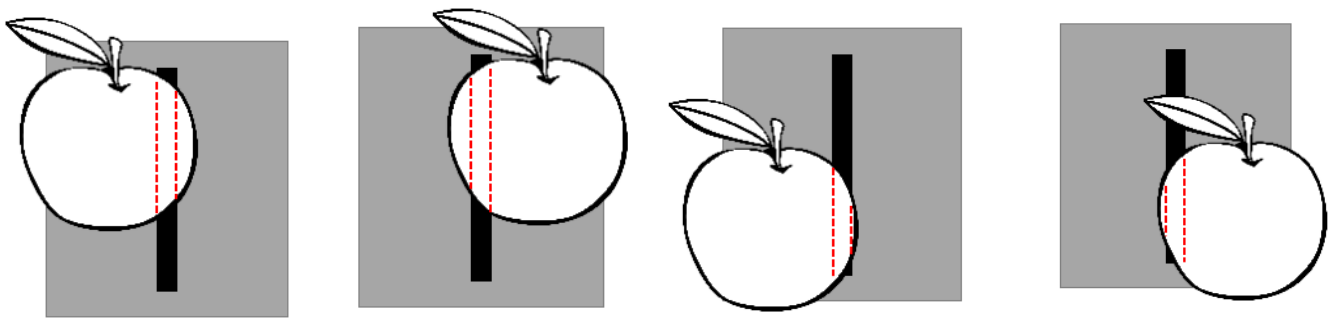

Figure 26. Representation of how the image of the simple moves along the focused plane, as well as the area that is measured at the same time.

Hence, the spectra obtained corresponded to a wide area, becoming useless to give each pixel a spectrum, since it wouldn't correspond to that point of the image, but to the mean of a lot of them.

After noticing the failure of the arrangement and what was causing those poor results, it was mandatory to find a solution.

The use of a pinhole that restricted the area of the object that was measured at once by the spectrometer was found as the best option to solve this major problem.

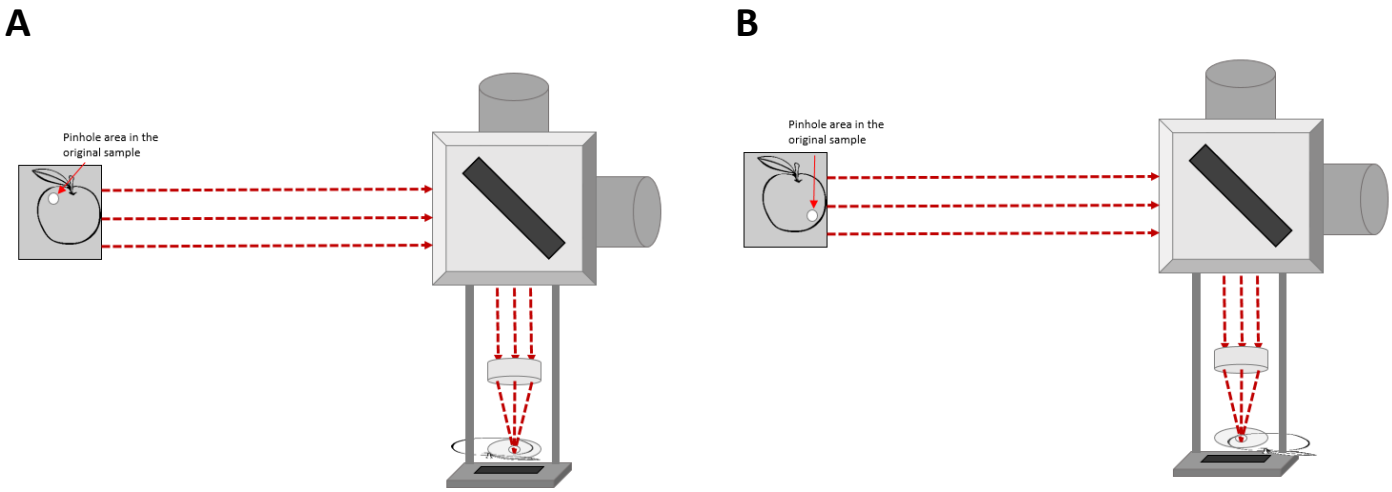

Figure 27. A: Area measured by the spectrometer in the sample B: Area measured after movement of galvo mirrors.

A Thorlabs diaphragm that allowed to control the size of the pinhole was used. It was placed immediately before the spectrometer.

With this improvement several problematic issues were solved.

- Instead of a wide area mas measured at the same time as before, only the light of a unique point of the sample was measured by the spectrometer.
- We have seen that the focused image moves along the plane of the spectrometer. Using the pinhole, we make sure that the light always arrive to the same point of the slit.

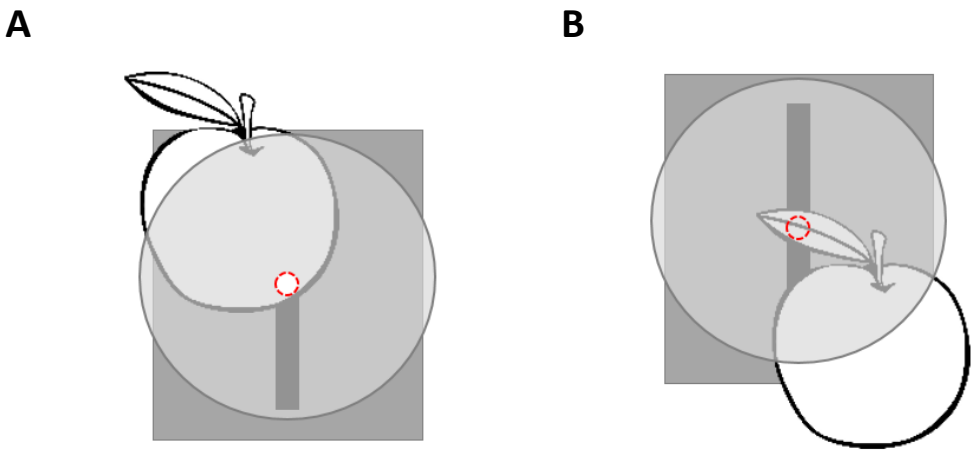

Figure 28. A: Area of the sample measured by the spectrometer. B: Area of the sample measured by the spectrometer after the movement of galvos.

I performed several tests with B&W images using this arrangement and the results obtained were favourable. It seemed that all the previous problems were surpassed. But when it came to colour images, results were a little bit difference. Due to the own arrangement of the spectrometer itself, it is required that the whole slit receives light. Otherwise, the spectrum obtained would be constrained to the region of the spectrum relative to the region of the slit that receives light. This wouldn't matter if the x-axis containing the values of λ was constrained at the same rate, but it isn't.

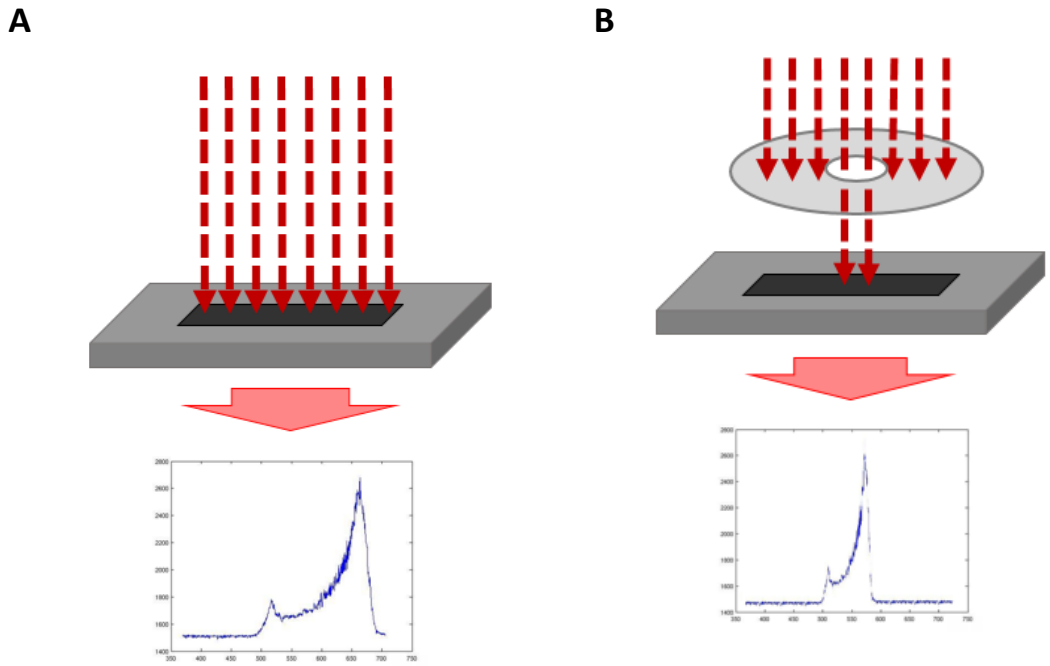

Figure 29. . A: Example of spectra obtained when the whole slit receives uniform light Vs. B: The spectrum obtained using a pinhole.

As it is seen, the spectrum in both cases gives the same information. But in the second one, it is adapted to the region of the slit that received light, leaving the rest of the spectrum as a flat signal. Hence, the intensities corresponding to each wavelength didn't match, making it impossible to know the real intensity values for each λ.

Since within Black and White images we are only interested in the integer of the whole spectrum of each pixel, that gives us an intensity value that moves in the range of white and black, it wasn't trivial to know the exact intensity values for each λ, but in colour images, it is essential to know the exact distribution of λ along the x-axis, in order to be able to separate the spectrum at specific λs at will.

This problem could be easily solved by dispersing the light along the whole slit length.

The SPARK-VIS spectrometer I used included an accessory specifically for this task. It is a piece that must be placed before the slit, with a small entrance for the light, and inside it has a lens that disperse it exactly to the size of the slit, as shown in figure XX.

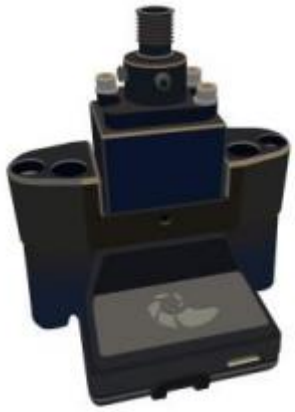

Figure 30. SPARK-VIS with light dispersion accessory attached

The adapter is magnetically attached to the front of the spectrometer. A fibre optic can be coupled to it, receiving the light of even a smaller region from it.

Theoretically, this would be more than enough to surpass that comeback, but in the practical issue, results were a bit different.

All the spectra collected didn't give any kind of information, it was just background signals, not the actual signal of the light received.

The last possible option that could lead to the success in this task was to use two extra lenses. A biconvex lens and immediately after a cylindrical lens.

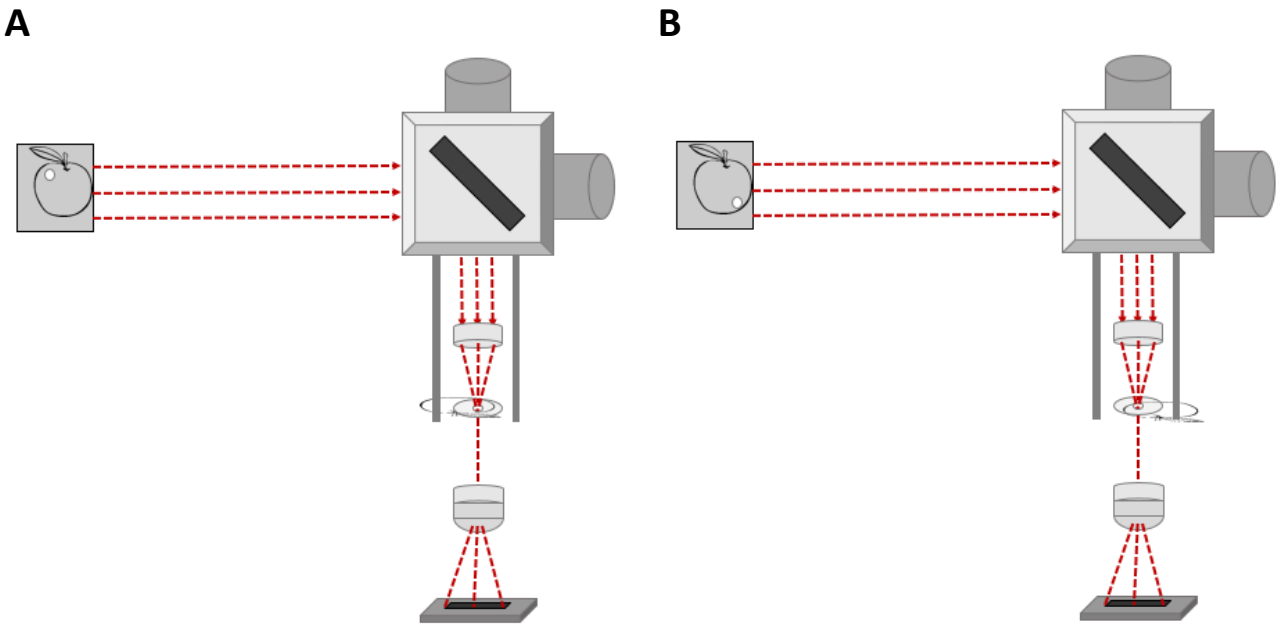

Figure 31. A: Dispersion of the light of the pinhole area along the whole slit. B: Same procedure after movement of galvo mirrors.

The second biconvex lens, placed at its focal length f=30mm from the pinhole, is used to focus again the image on a new point. Since we are trying to avoid for the image to be focused on a single point, the arrangement of the cylindrical lens right after this second biconvex lens solve the problem.

This final arrangement allow us to disperse all the receiving light in a straight line that covers the whole slit of the spectrometer, and this is the status at which we performed the experiments.

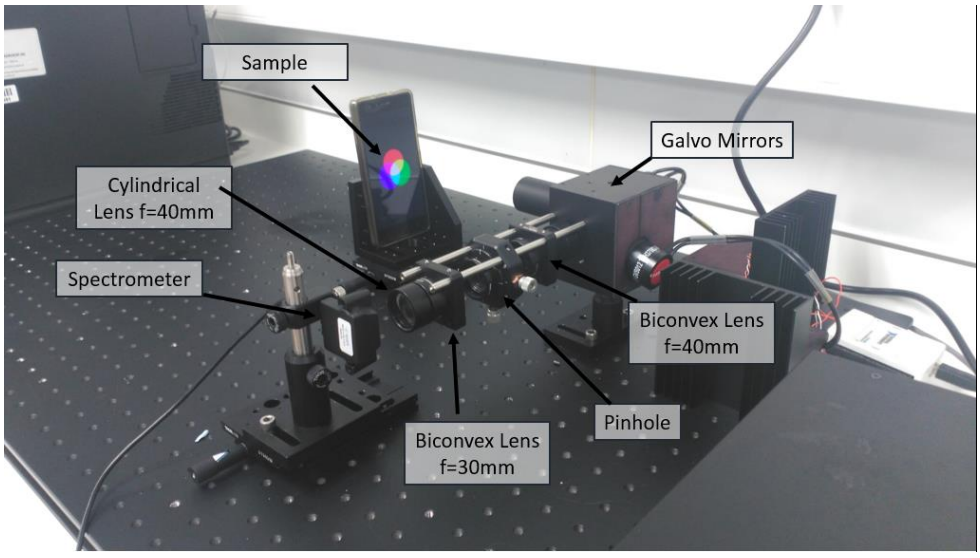

Figure 32. Actual arrangment of the system

5. Software development

All these devices can't work without a proper software with which they can communicate. It was highly advisable that all devices could be controlled at the same time, regarding that they come from different companies. LabVIEW was the software selected for this task, and for the analysis part Matlab was the best option.

5.1. LabVIEW program

LabVIEW is a development environment for visual programming language. It is commonly used for data acquisition and instrument control. LabVIEW programs are called virtual instruments (VIs), and they can be called between each other, working as a bigger VI that depends on smaller ones. Each VI contain two components: A block diagram and a front panel.

All the programming is done in the block diagram, it contains the source code. All the structures and functions, as well as other VIs, are placed and performed in the block diagram.

The front panel is built with controls and indicators. It is the interface by which you control the programming on the block diagram. You can give inputs to the program, receive results... [25]

I have used the latest version of LabVIEW, LabVIEW 2015 (64-bit), and several steps were followed in order to fulfill the task of controlling Galvo mirrors and making all the measurements. The first step taken was to perform both tasks independently.

For the control of the Galvo mirrors I first had to install the NI-DAQmx driver software, in order for the computer being able to detect the hardware device. Once it was installed, new available VIs were created that could be used in LabVIEW to create a flow of information between the DAQ and the computer. For the control of the mirrors you

needed to introduce 4 inputs: The voltage in the *x* and *y* direction (0-5V), which will determine the size in both directions covered by the mirrors, and the increment in voltage in both *x* and *y* that will determine the distance covered between one measurement and the next one.

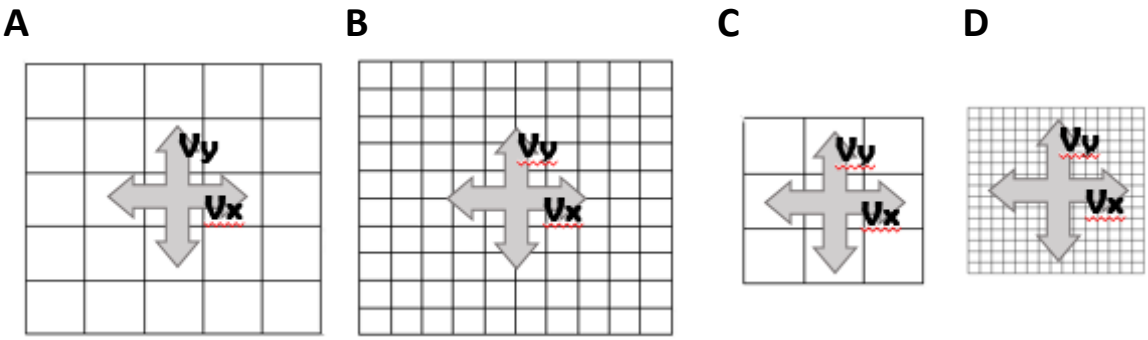

Figure 33. Different scanning performance of the galvo mirrors as a function of the inputs given.

A. X-Axis= Y-Axis= 5V X-increment=Y-increment=1 V
B. X-Axis= Y-Axis= 5V X-increment=Y-increment=0.5 V
C. X-Axis= Y-Axis= 3V X-increment=Y-increment=1 V
D. X-Axis= Y-Axis= 3V X-increment=Y-increment=0.2 V

The other task consists in the control of the spectrometer. For this issue another software needed to be installed, in order for the computer to recognize the spectrometer. Omnidriver is an Ocean Optics software that allow to create new software intended to interact with Ocean Optics spectrometer. It can be used in several different programming languages, including LabVIEW. Once it is installed a lot of different VIs are created in the computer that can be used by LabVIEW and are specific for the control of the spectrometer. Each VI perform a different task in the process of spectra acquiring. These tasks include: Open the spectrometer, get the wavelength range (in our case 380-700nm), set integration time, get the spectrum and close the spectrometer. In this case, only one input is required, which is the integration time. This value states how many time the spectrometer is going to keep measuring light to obtain the spectrum. The longer the integration time, more signal it will receive and better results will be obtained. Longer integration times will be required when the measurements are performed in dimmer places.

Once these tasks were under controlled independently, they had to be performed at once and in a rigorous way and controlling all of them from the same interface. With these purpose, flat sequence structures were used. Flat structures are divided in different boxes, and in each box it can be assigned a function. The boxes will start working from left to right. Once the performance of the task of one box is finished, it will begin the performance of the task of the following box, and not before. Moreover, using while loops, this process is repeated as many times as number of measurements are performed, i.e. the number of pixels.

The whole process of spectra acquiring is performed within the VI Galvo_Mirrors_Main, in which other VI are called:

- Omnidriver_init, it opens and initialize all the spectrometers connected to the computer
- Galvo_Mirrors_Scan, it performs the organized process of moving the mirrors, measuring the spectra, and store all the spectra in a folder of the computer of your choice.
- Omnidriver_read (Used inside Galvo_Mirrors_Scan), it measures the spectrum acquired by the spectrometer.
- Omnidriver_close, it closes all spectrometers connected to the computer.

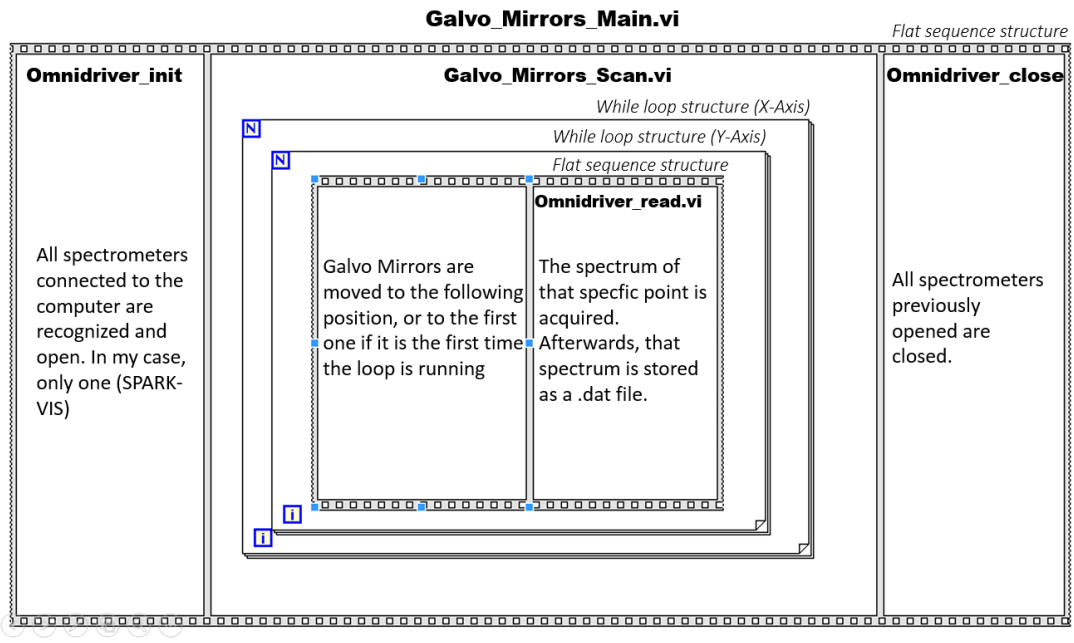

Figure 34. Simplified representation of the program.

But, in the end, the user will only see and interact with the interface created in the front panel of the main program.

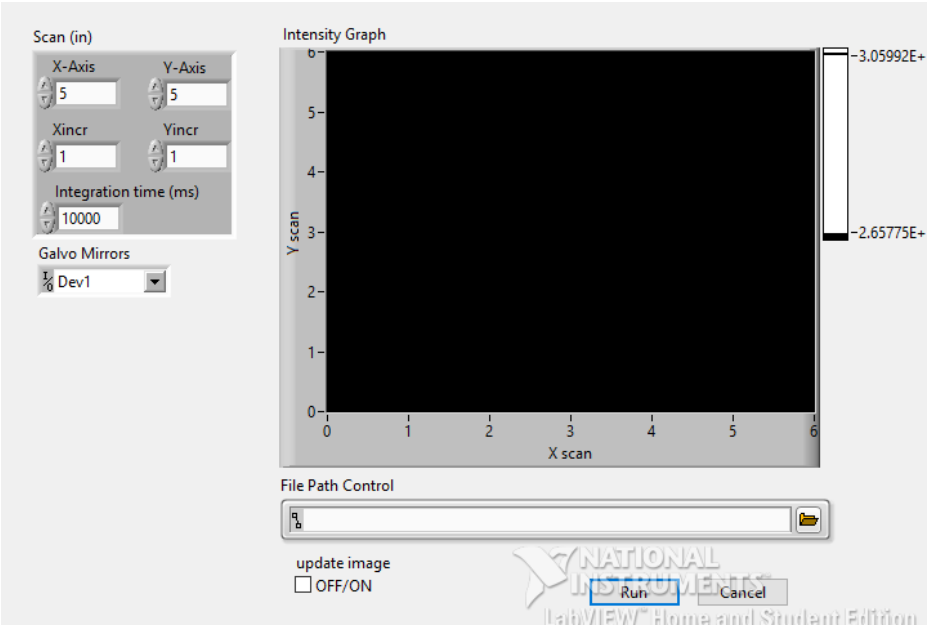

Figure 35. Interface of Galvo_Mirror_Main.

In this interface you can control the whole process of spectra acquisition. You have eight inputs and one output.

The eight inputs correspond to: size of X-axis, size of Y-Axis, resolution of X-Axis (Xincr), resolution of Y-Axis (Yincr), integration time (in ms), spectrometer used, in my case only option is SPARK-VIS, file path, in which you stablish where do you want to store all the .dat files corresponding to all the spectra and an option of continuously updating an image (Y/N). In the case of selecting the box, the program will keep running indefinitely and updating the image.

The output we have correspond to the image obtained. It is shown in blue-scale and it is merely shown to see the quality of the image acquired, since the analysis of the images will be done in matlab.

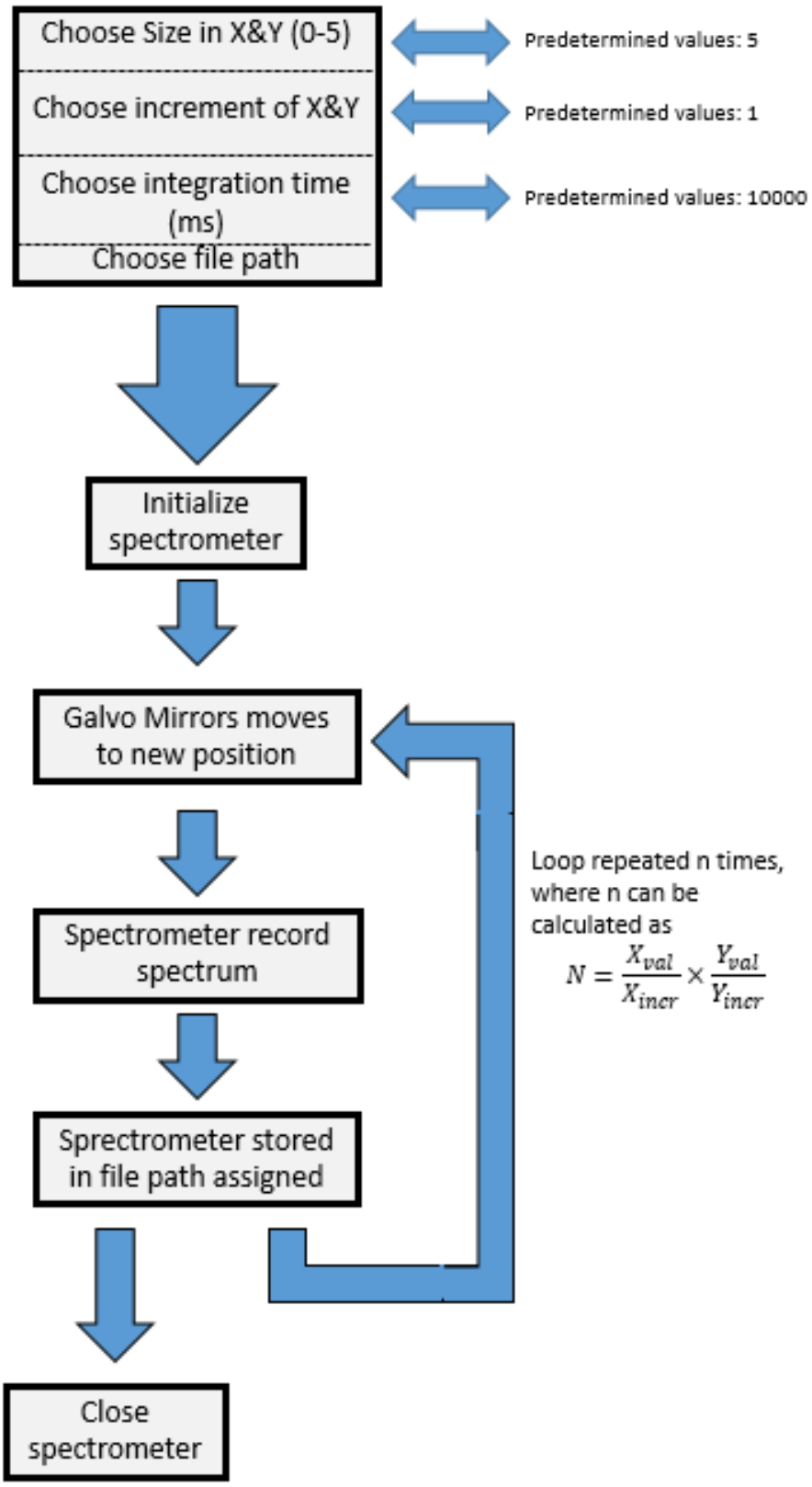

Figure 36. Scheme of the performance of the hyperspectral imaging acquisition.

5.2. Data processing

Once all the spectra are acquired, they are stored in the same order as they were taken in the file you stablished. Now, all these spectra must be processed. There are plenty of software to perform this processing, I have used Matlab, since it is a software I have worked a lot with during this last years, and provide more than enough tools to perform this data analysis.

The first step is to open all spectra acquired with the spectrometer with Matlab. Once this is done, it is necessary to store them in a matrix that later on will form our image.

After having all spectra arranged in a 2D matrix, the data processing begins. First, correction and calibration must be performed. For this, calibration and background spectra will be needed.

As it was previously stated, correction of the spectrum is performed by subtracting the background information from the spectrum measured in each point.

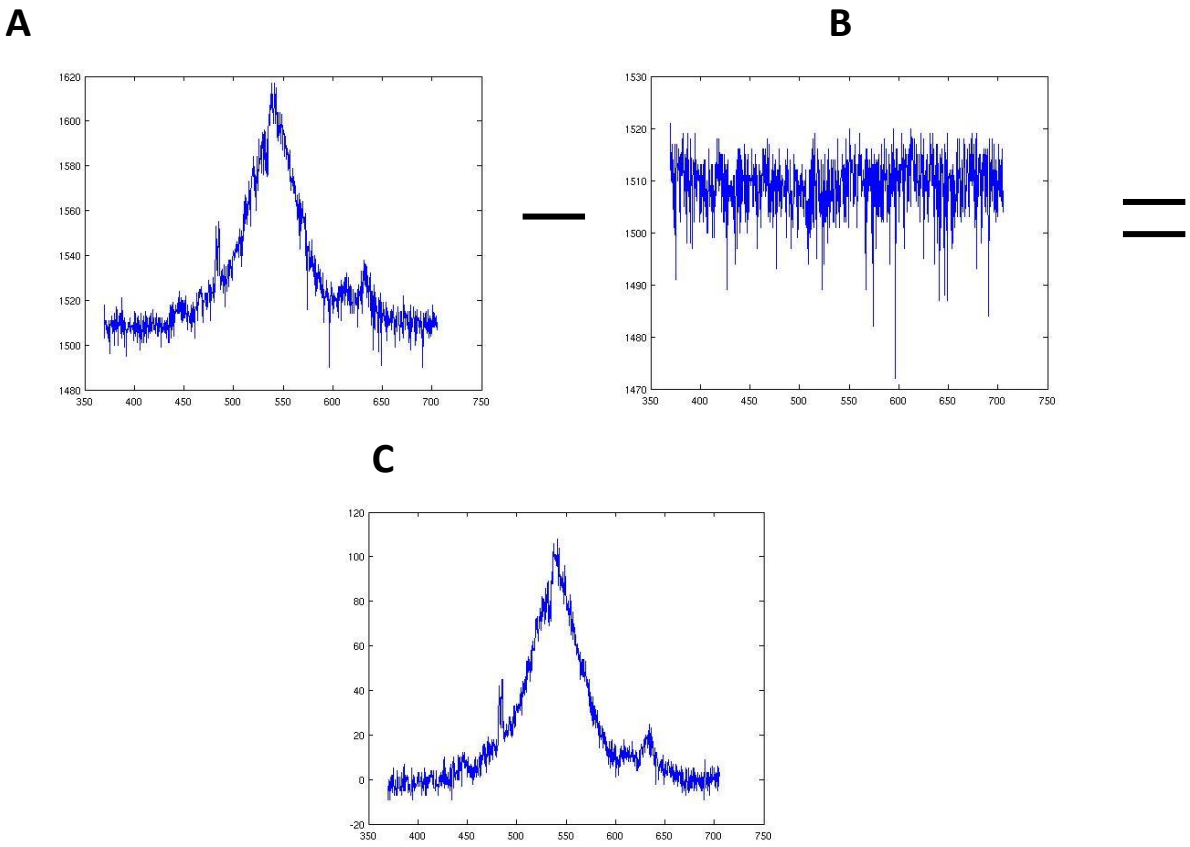

Figure 37. A: Raw spectrum acquired. B: Background spectrum. C: Corrected image.

It is seen that corrected spectra are smoother, without less unexpected peaks.

The next step is to perform the calibration step. Some problems aroused when performing calibration, due to technical flaws in the arrangement of the system. Still, the results obtained just by performing correction are excellent, so we didn't hesitate to finish this section.

The problem appeared when performing the spectral acquisition of the halogen light of the calibration lamp. For all points of the image, a calibration spectrum should be measure, and in theory all these spectra should be the same. However, the difference among them stated that this doesn't happen. Some of them are so poorly reliable to the theoretical one that they get rid of important information on the spectra, such as entire ranges of colour.

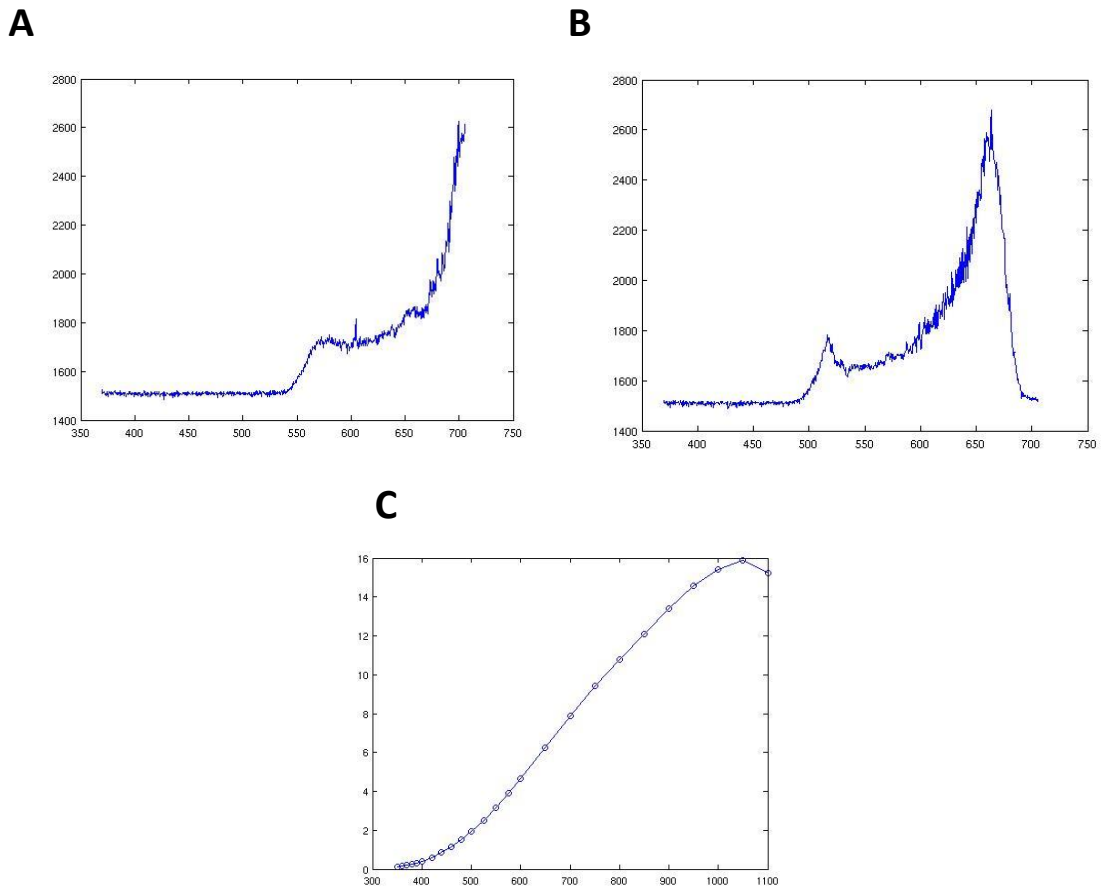

Figure 38. A&B: Different calibration spectra measured at differnet position of the galvo mirrors. C: Theoretical halogen lamp calibration sprectrum provided by the company.

Nevertheless, I find important to explain how calibration is performed, for future implementations.

At this point we will have a matrix composed of corrected spectra. Having this we, I have followed two paths that lead to two different results. Depending on the application of the system, one of them may be a better approach.

The first path to follow is intended to experiments in which light emission intensity is the key factor, independently of the colour of that emission. In order to find the intensity value of a pixel, we must perform the integer of the spectrum along the whole visible range.

$$I(i,j) = \int_{\lambda_0}^{\lambda_f} S_{\lambda}^{corr}\, d\lambda$$

Where λ_f is the last wavelength value of our spectrum and λ_0 the first one (In our case, 700nm and 380nm respectively.

The resulting matrix will contain the intensity values that correspond to every pixel. The resulting image is a binary image that shows the differences in intensity of the sample measured.

The other possible path follows the hyperspectral approach, which is the one thought for this project. Spectrum can be separated in different λ ranges, for instance red, green and blue ranges.

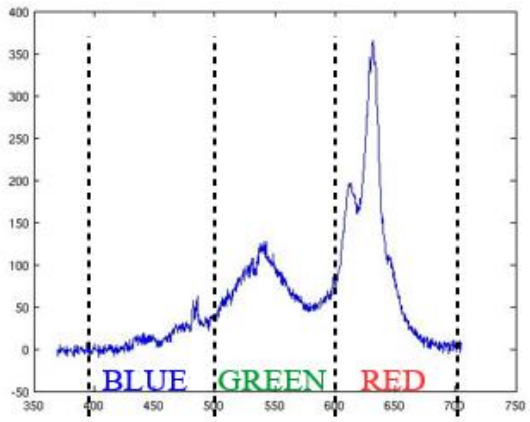

Figure 39. Colour ranges distintion

From each range we perform the integer, obtaining that way intensity values of different colors, in the case of separating it in the RGB ranges.

$$H(i,j) = \int_{\lambda_1}^{\lambda_2} S_\lambda^{corr}\, d\lambda$$

Corresponding λ_1 the first wavelength value of the range and λ_2 the last value.

All those intensity values are stored in a 3D matrix, the hypercube, where the new dimension added to our previous 2D corresponds to the hyperspectral ranges. The first range will be stored in the first layer, the second range on the second layer…

Since I have been working on the visible range, I have separate the spectra into the three ranges I have already mentioned.

Color	Left limit (nm)	Right Limit (nm)
BLUE	402	502
GREEN	502	601
RED	601	701

Table 2. λ limits of three ranges

Once we have our hypercube, the continuing of the processing depends entirely on the application it is intended to do. As a final step I have decide to create a color image of the sample measured. Since we already have the intensities of each range, we must find the values of each pixel. In a RGB color, each pixel is formed of three values (R, G, B). These values are found in a range between 0 and 255, and they can be easily calculated with the intensity values previously obtained.

$$R = \frac{R_i}{R_i + G_i + B_i} \times 255 \qquad G = \frac{G_i}{R_i + G_i + B_i} \times 255 \qquad B = \frac{B_i}{R_i + G_i + B_i} \times 255$$

The resulting image can be easily shown on Matlab.

6. Results analysis and Discussion

The reconstruction of images from the spectra acquired by the device proved to be a success. We have been able to obtain adequate spectra that fits the reality of the sample measured, and we have created a robust enough method that allow us to perform an approach in the matter of hyperspectral imaging.

The usefulness of both the hyperspectral device and the analysis method have been shown, and further development of both of them will derivate in the actual test in medical situations.

6.1. Imaging

For all the experiments I have performed the maximum scanning range in both X and Y direction, by applying a voltage of 5V in both of them. This way it has been easier to compute the processing and obtaining adequate results. From now on, consider that all the important values I provide are thought for the maximum optical scanning range of the system.

These were the first images we successfully were able to measure and reconstruct. It was the very first approach and it proved that the theoretical idea of the project was reliable on the practice.

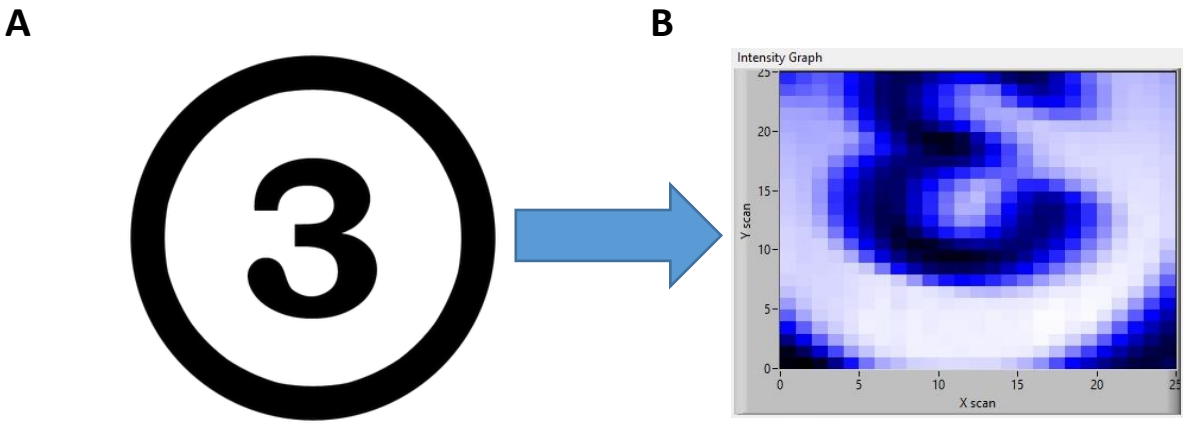

Figure 40. FIrst image succesfully acquired with the system.

This image was obtained with the arrangement of the pinhole, without using the cylindrical lens. Therefore, spectra were not accurate in the sense of wavelength/intensity values, but more than enough to obtain a single intensity value per pixel and obtain a raw image.

The first image obtained with the final arrangement was B&W as well.

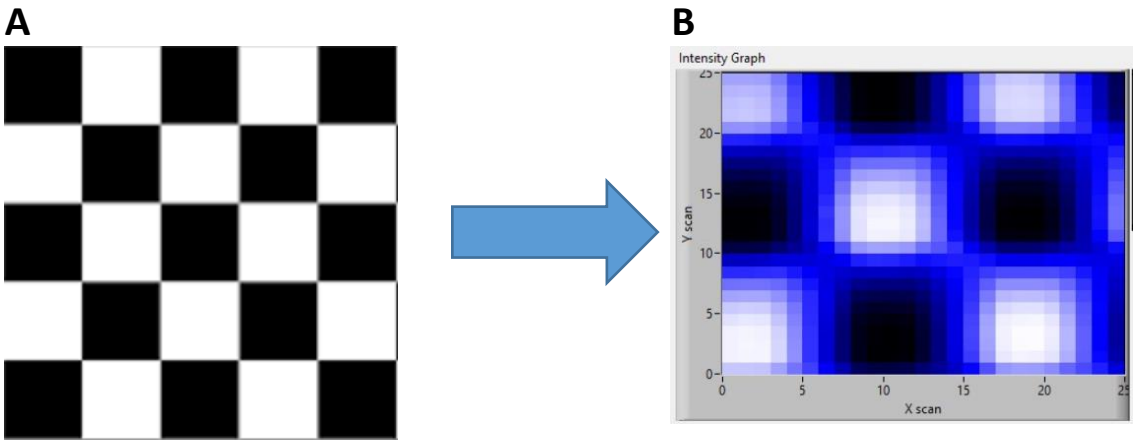

Figure 41. Fiirst image sucesfully acquired with the final optical arrangement. A: Original image. B: Acquired image

Using a checkerboard was useful to calculate several things.

First, the field of view (FOV) of the device. Regarding that each square had a length of 1.25cm, that between the centers of two squares in the reconstructed image there are 9 pixels, and that there is a total of 25 pixels in both directions, we can find that the FOV is

$$FOV = \frac{1.25}{9} \times 25 = 3.5\ cm$$

The actual size of the sample recorded images will be 3.5x3.5 cm, with a pixel size of 0.139cm.

It is observed that the edge distinction between squares is poor. This is due to the fact that the pinhole covered an area bigger than it should, but making it smaller, not enough light would get to the spectrometer for it to be measured. Moreover, the integration time applied to the spectrometer will affect resolution as well. Longer integration times will acquire more accurate spectra, but of course increasing the scanning duration. Hence, there is a need to find the best equilibrium between sacrificing resolution over a better signal acquisition and scanning duration. For this test, the diameter of the pinhole was fixed with a diameter of 1mm and the integration time at integration time of 100000 μs (10^{-6}s). In order to find the actual area of the sample that mas measured at each point, it is needed to know the magnification factor of the system (M). It is calculated knowing the focal length (f) of the first lens and its distance to the sample (S_1)

$$M = \frac{f}{f - S_1}; \quad M = \frac{40}{40 - 270}; \quad M = -0.174$$

There is a convenience of giving it as a negative value due to the fact that the image is rotated within the lens. An M lower than 1 means that the image is actually reduced in size. Hence the pinhole placed at the image formed after the lens will cover a total area of 26mm^2. That corresponds to a huge area in order to measure the value of a single pixel. Future development may solve this drawback.

6.2. Hyperspectral imaging

Once, the cylindrical lens was arranged, there is no difference between scanning B&W and color images. The results have been highly satisfactory. In order to prove the accuracy of the results and the efficiency of the method we decided to use an image with easily differentiable bright colors.

Figure 42. Image used to perform the anaylsis for the results

This is the image used to perform all the analysis and reconstruction procedures. I have performed this experiment twice, once with a voltage resolution (related to the galvo mirror functionality) of 0.2V and another time with 0.1V. The integration time was fixed for both of them (100000 µs). The first one had a total scanning time of 1:30 mins, while the second one of 6:05mins. It is going to be shown all the imaging steps and the results in the hyperspectral approach.

The first image obtained when scanning a sample is the binary one provided by LabVIEW. It gives you a first idea of how the scanning went. In this image it can be observed that the basic shapes, such as the circles, and the areas with highest intensity, the white center, are easily differentiable.

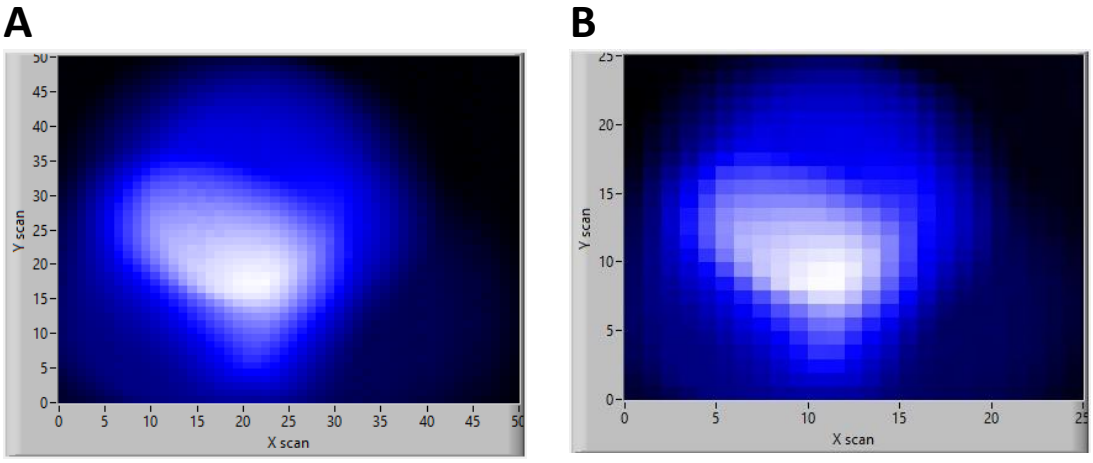

Figure 43. First approach of the acquised image provided by LabVIEW A: Resolution of 0.1 V B: Resolution of 0.2 V

Once we start working on Matlab and performing the hyperspectral step, we can see how the three color circles are perfectly delimited, with higher intensities in the areas with the pure color and lower intensities in the areas where circles overlap.

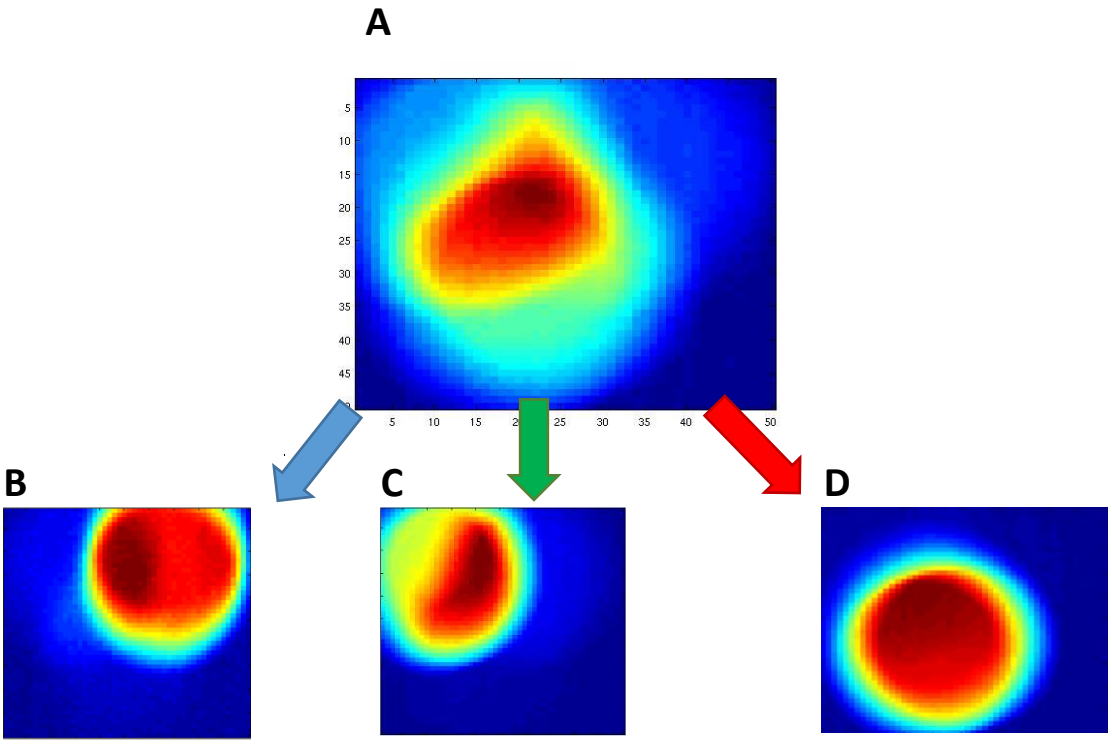

Figure 44. A. Intensity image of the whole spectrum. B: Intensity image in the blue range. C: Intensity image in the green range. D: Intensity image in the red range

Moreover, it has been demonstrated the accuracy of the method in obtaining real spectrum of the incoming light. By comparing single color area spectrum and mixed color areas spectrum, we can see that the latter ones correspond to the sum of single color ones. I consider this as the most important proof that the system works.

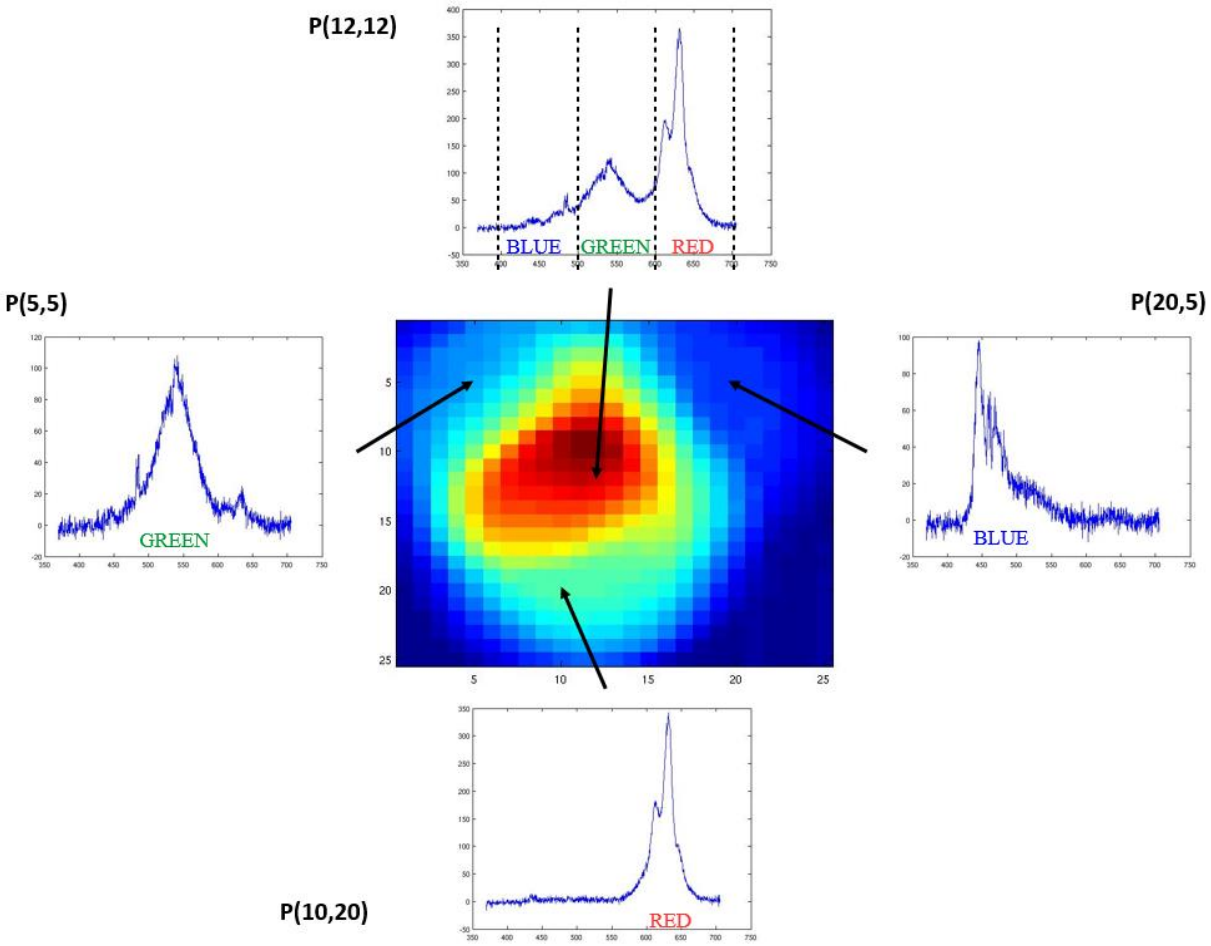

Figure 45. Spectral distribution of colours along the whole spectrum

A corresponds to the spectrum obtained at the centre (white). B, C and D corresponds to spectra obtained far from the centre and corresponding to a specific colour disk. Theoretically, the sum of the latter ones should give us the white colour spectrum. After performing this operations, these are the results

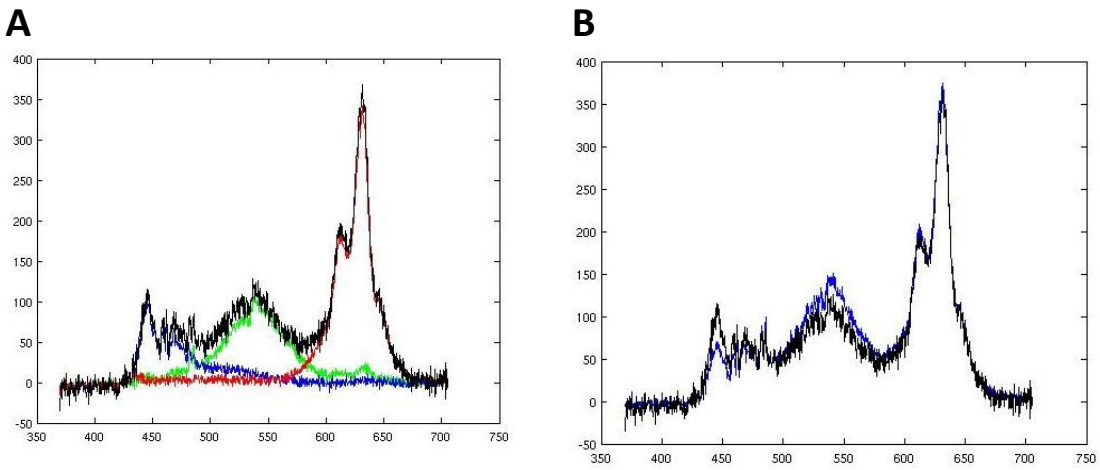

Figure 46. A: Sum of spectra of different light colours. B: Comparison of the calculated spectrum and the measured one

Plot A shows in the same axis the spectra of the three different colours and the sum of the three of them (black). Plot B shows the comparison of that sum with the actual spectrum measured at the centre (blue).

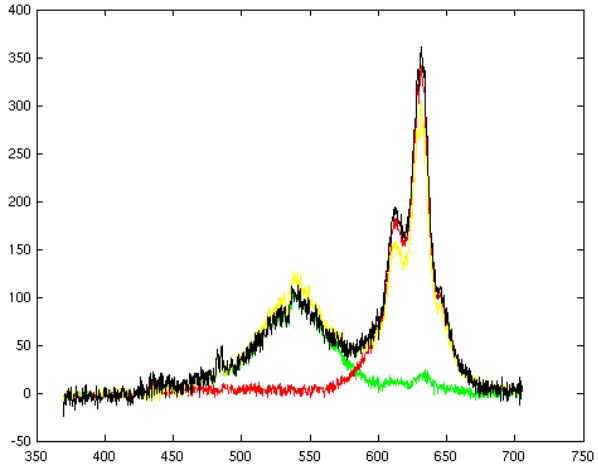

Figure 47. Sum of red and Green spectra, giving arise to yellow spectrum.

The same procedure performed in the overlapping zone of red and green disk, corresponding to yellow. The black spectrum correspond to the actual one measured in that area, while the yellow one is the sum of green and red spectra. The same analysis can be performed in the region where blue and red disks and where green and blue disks overlaps

It is seen in both examples that the spectrum obtained with the sum of different ranges spectra fits almost perfectly the one measured by the spectrometer. Moreover, it is demonstrated as well that spectrum doesn't change in an area with the same colour.

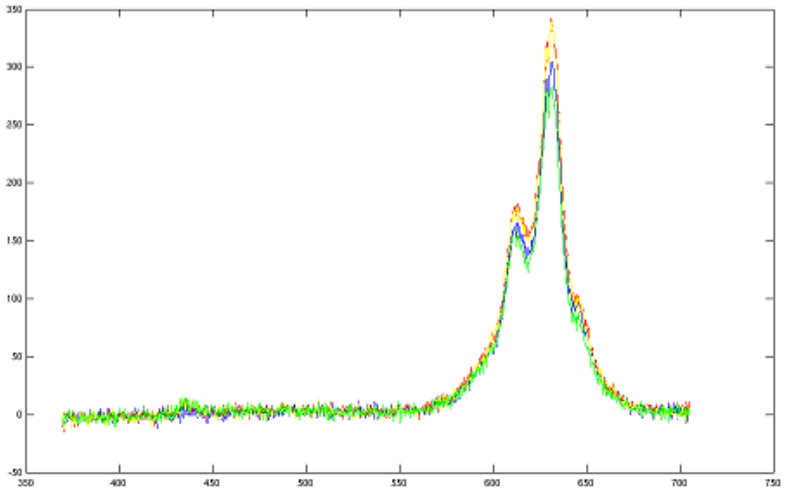

Figure 48. Comparison of spectra in different points of the same color disk (red)

These are the spectra of four different points in the red disk. The accuracy of the system is observed in the fact that there are minimal changes among them.

Although the provided results have been only worked on the visible range, in order to being easier to understand, there is no limitation in the ranges selection in the spectrum. Let's take for instance that you are studying the fluorescence in a tissue that emits light in the green range. With these system you can make the acquisition, get rid of the parts of the spectrum we are not interested in and show in an image only the areas where fluorescence is present. The development of the system in certain areas can suppose a great advancement in diagnosis imaging techniques.

Once this is done, the recovery of the colour image is not so complicated.

Although of course it is not extremely accurate, it is seen a high resemblance to the original image.

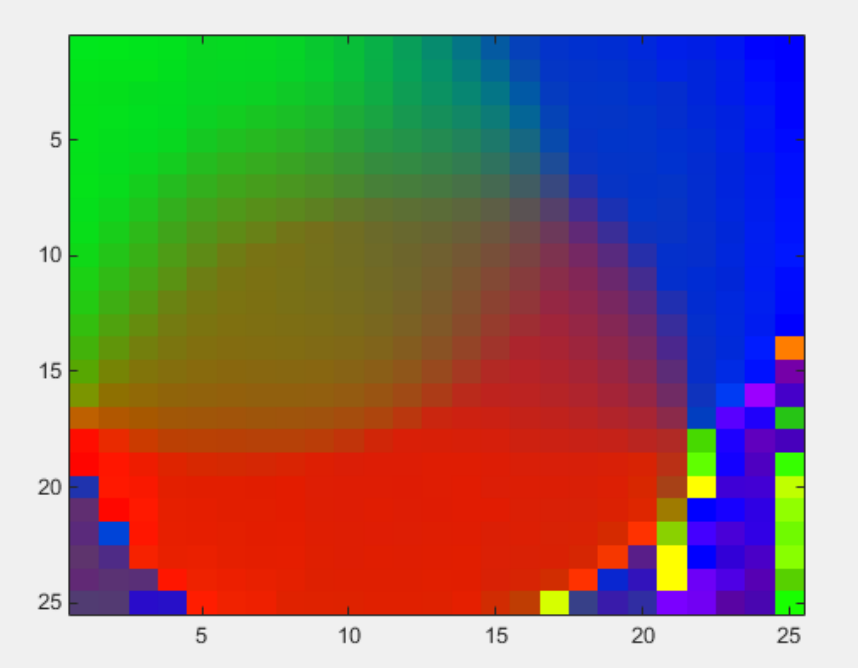

Figure 49. Reconstructed image colour

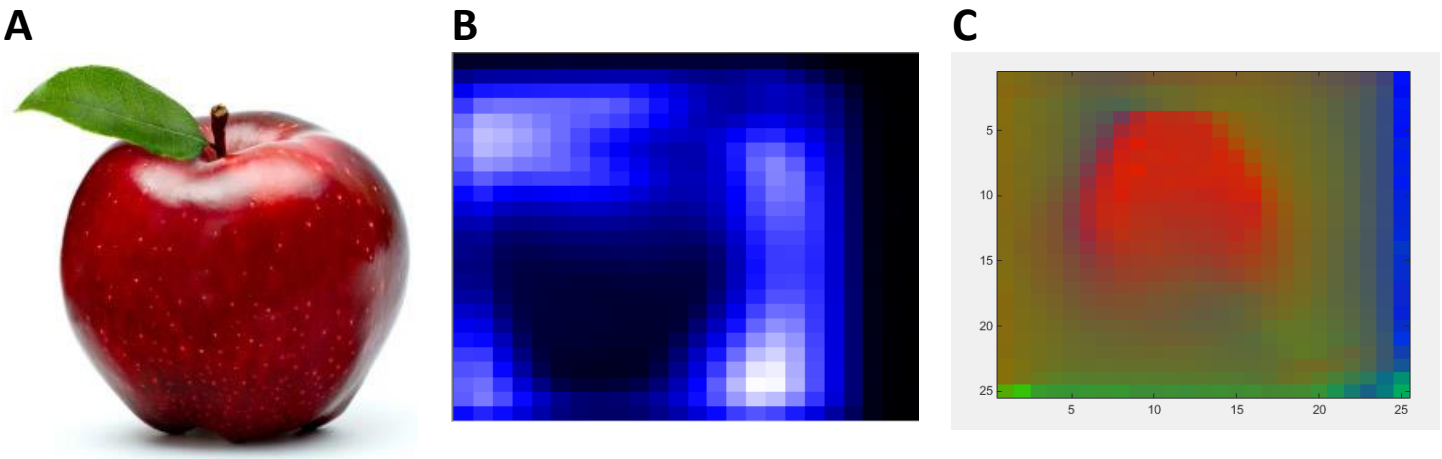

Figure 50. Another hyperspectral analysis performance. A: Original Image. B: Binary Image processed by LabVIEW. C: Reconstructed image.

It is observed a lateral inversion between the original image and the binary one. This is due to the arrangement of lenses and the movement of galvo mirrors. Afterwards this image is turned upside down, resulting in an image turned 180º with respect to the original one.Nevertheless, this doesn't suppose any critical change in the results.

7. Conclusions and perspectives

7.1. Concluding remarks

A hyperspectral imaging system has been developed and improved in its first stages during the project. The design and arrangement of a functional optical system has been successfully carried on, as well as the creation of a program intended to analyze and process the data previously obtained.

The creation of a highly precise system that allow us to control several instruments at once in a perfectly structured path has been a success. The movement of the galvo mirrors in relation with spectrum acquisition is the main technical basis at which this project relies on.

We have succeed as well in the control all the parameters needed to adapt the system to a specific experiment. Integration time of the spectrometer, Field of view of the galvo mirrors… the freedom to change these values at will makes this system more reliable.

It has been proved that the results obtained, both in binary and colour images, are as expected, and fulfils the requirements of hyperspectral imaging technology.

Nevertheless some problems that aroused along the project has made impossible to perform some improvements initially projected. The loss of signal when using an optical fiber fixed to the spectrometer has been the major one. It has made us reconsider the whole optical arrangement, sacrifying some aspects such as a good resolution.

Still I am pretty confident that this project will be helpful in the future in the medical application of hyperspectral systems.

7.2. Future work

The continuity in the development of the system as well as of the data processing software would be the next steps in this project.

The first step needed to get better results should be changing the spectrometer. The one used until now have some important flaws that are hardly solved. Ocean optics has a wide offer on spectrometers that can be used with the already existent LabVIEW program.

Find a method to improve the arrangement of the optics, in order to avoid drawbacks such as the one on the calibration procedure.

Change the position of the lenses to perform a magnification of the sample, in order to reduce the actual area covered by the pinhole, in order to increase resolution. For this task, the lens should be place nearer the sample and further from the pinhole.

Perform some scanning of a non-self-illuminated surface, using an external source of illumination.

Perform, first in vitro, and afterwards in vitro tests that show the efficiency of the technique.

A possible future approach could be the arrangement of a motor below the sample to study that works together with the galvo mirrors and spectrometer, allowing us to obtain 3-dimensional images of our sample in the hyperspectral range.

Project Costs

The budget of the project was calculated taking into account three types of resources: Hyperspectral system components, technical equipment and human resources.

Hyperspectral system components	Quantity	Costs/Units	Total Cost
GVS012 - 2D Large Beam (10 mm) Diameter Galvo System, Silver-Coated Mirrors. Thorlabs inc, Delaware, USA.	1	2,538.10 €	2,538.10 €
GPS011 - 1D or 2D Galvo System Linear Power Supply. Thorlabs inc, Delaware, USA.	1	405.00 €	405.00 €
GCM012 - 30 mm Cage Adapter for 10 mm Galvo System. Thorlabs inc, Delaware, USA.	1	162.00 €	162.00 €
AC254-040-A-ML - f=40 mm, Ø1" Achromatic Doublet, SM1-Threaded Mount, ARC: 400-700 nm. Thorlabs inc, Delaware, USA.	1	86.31 €	86.31 €
AC254-030-A-ML - f=30 mm, Ø1" Achromatic Doublet, SM1-Threaded Mount, ARC: 400-700 nm. Thorlabs inc, Delaware, USA.	1	91.80 €	91.80 €
LJ1695RM-A - f = 50 mm, Ø1", N-BK7 Mounted Plano-Convex Round Cyl Lens, ARC 350-700. Thorlabs inc, Delaware, USA.	1	89.10 €	89.10 €
SM1D12 - SM1 Lever-Actuated Iris Diaphragm (Ø0.8 - Ø12 mm). Thorlabs inc, Delaware, USA.	1	50.13 €	50.13 €
CP02/M - SM1-Threaded 30 mm Cage Plate, 0.35" Thick, 2 Retaining Rings, M4 Tap. Thorlabs inc, Delaware, USA.	2	14.40 €	28.80 €
CXY1Q - 30 mm Cage System, XY Translating Mount for Ø1" Optics with Quick Release Plate. Thorlabs inc, Delaware, USA.	1	202.50 €	202.50 €
USB-600914-Bit, 48 kS/s Low-Cost Multifunction DAQ. National Instruments Corporation, Texas, USA.	1	395.00 €	395.00 €
DH-2000 Deuterium-Halogen Light Source. Ocean Optics Inc, Florida, USA.		3,200.00 €	3,200.00 €
Spectrometer: Spark-VIS. Ocean Optics Inc, Florida, USA.	1	415 €	415 €
		Total=	7,663.74 €

Table 3. HSI system components costs.

Technical equipment	Quantity	Costs/Units	Total Cost
OmniDriver, Cross-Platform Full-Featured Device Driver. Ocean Optics Inc, Florida, USA.	1	500.00 €	500.00 €
LabVIEW Software (free student version). National Instruments Corporation, Texas, USA.	1	600.00 €	600.00 €
Matlab Softwar. The Mathworks Inc, Masschusetts, USA	1	500.00 €	500.00 €
		Total=	1,600.00 €

Table 4. Technical equipment costs.

Human resources costs comprise the salaries of the team members working on the project. In this case, the student, the tutor and the Co-tutor worked full. I consider an average salary for the student of 25€/hour and an average salary for the tutor and co-tutor as engineer of 40€/hour.

Human resources	Months	Cost/month	Total
Student	8	750 €	6,000 €
Tutor	8	1,200 €	9,600 €
Co-tutor	8	1,200 €	9,600 €
		Total=	25,200 €

Table 5. Human resources costs

Concept	Total cost
Hyperspectral system components	7,663.74 €
Technical equipment	1,600.00 €
Human resources	25,200 €
Total=	34,463.74 €

Table 6. Total costs.

ANNEX

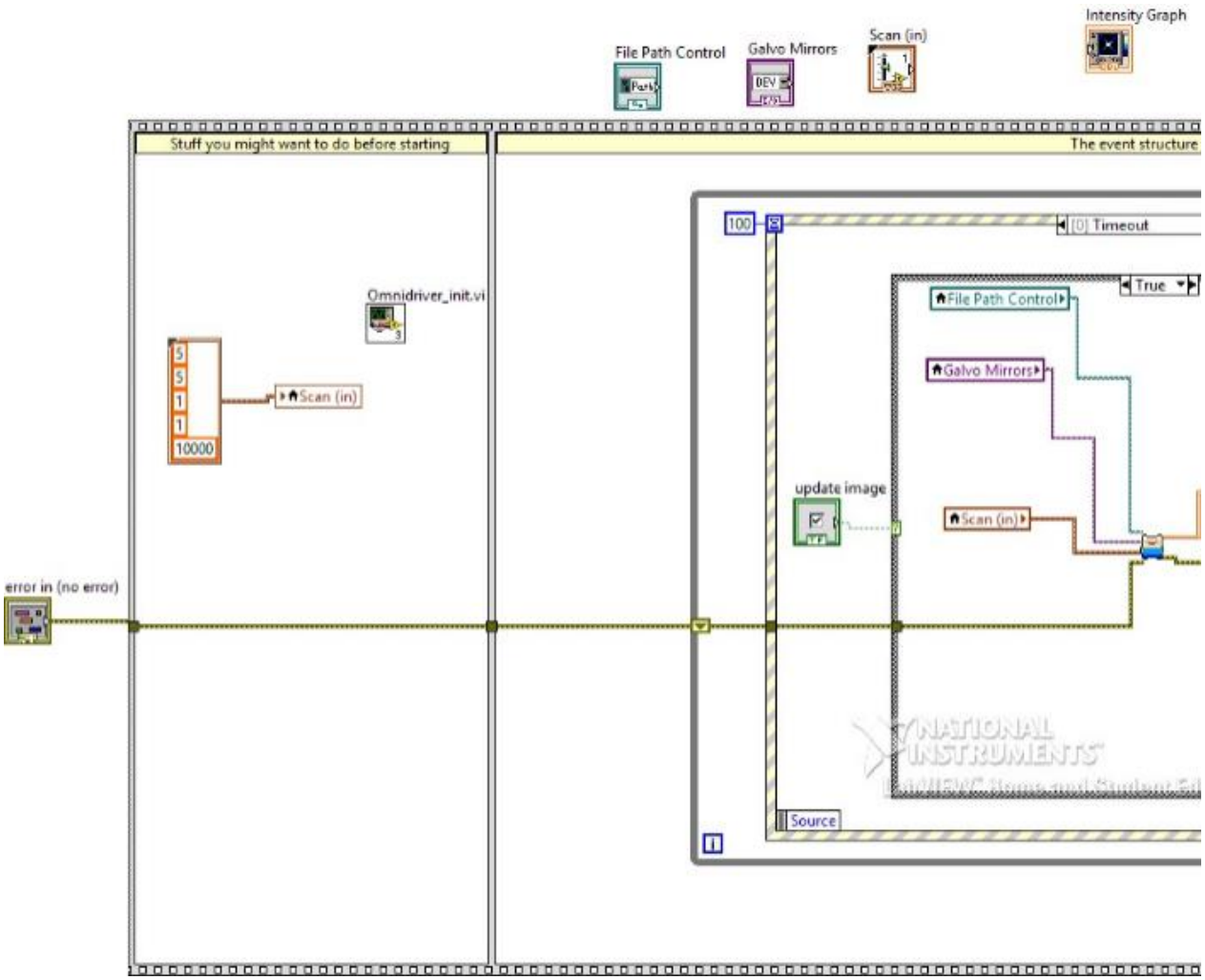

Figure 51 Terminal window of galvo_mirror_main LabVIEW program

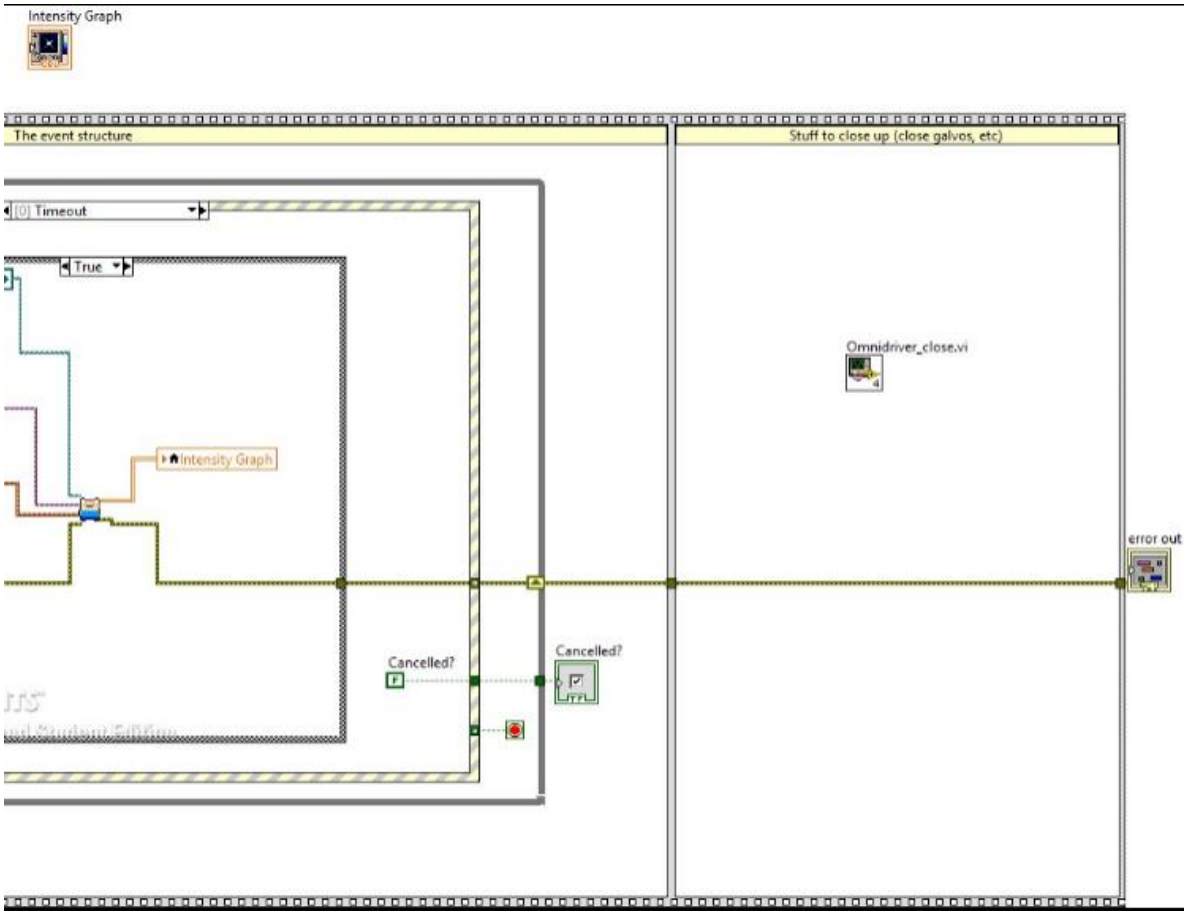

Figure 52. Terminal window of galvo_mirror_main LabVIEW program

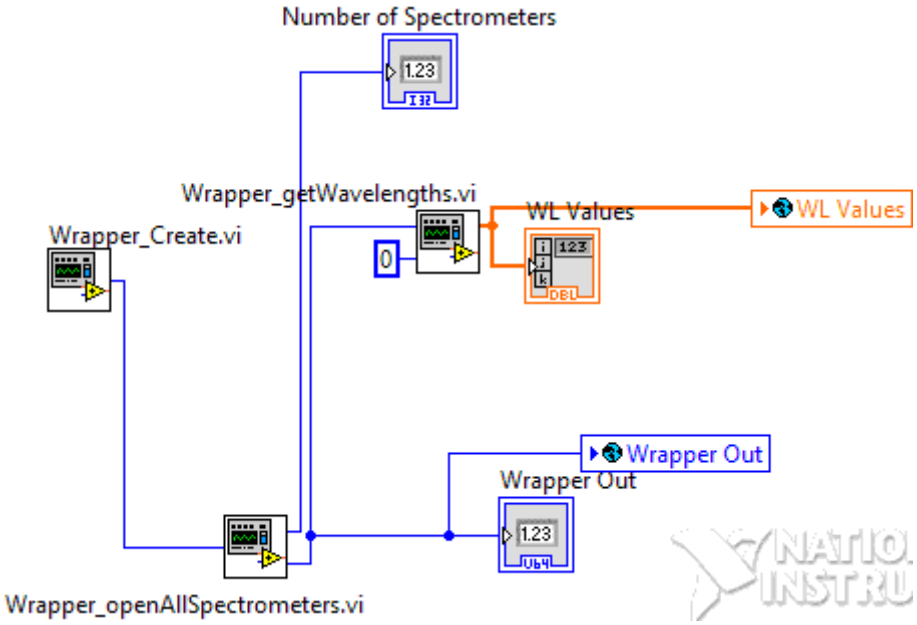

Figure 53 Terminal window of omnidriver_init LabVIEW program

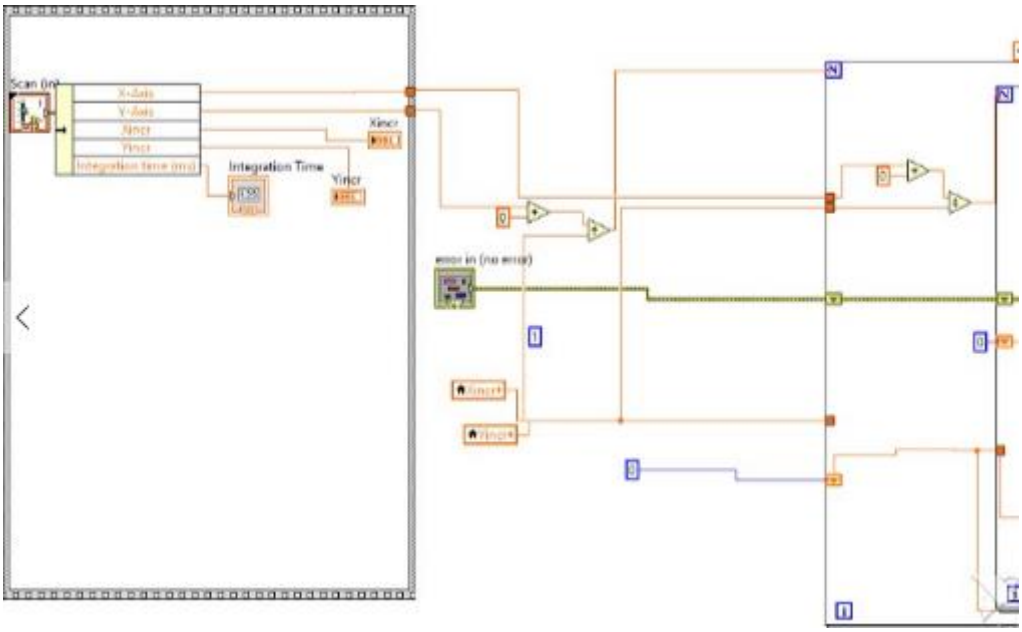

Figure 54. Terminal window of galvo_mirrors_scan LabVIEW program

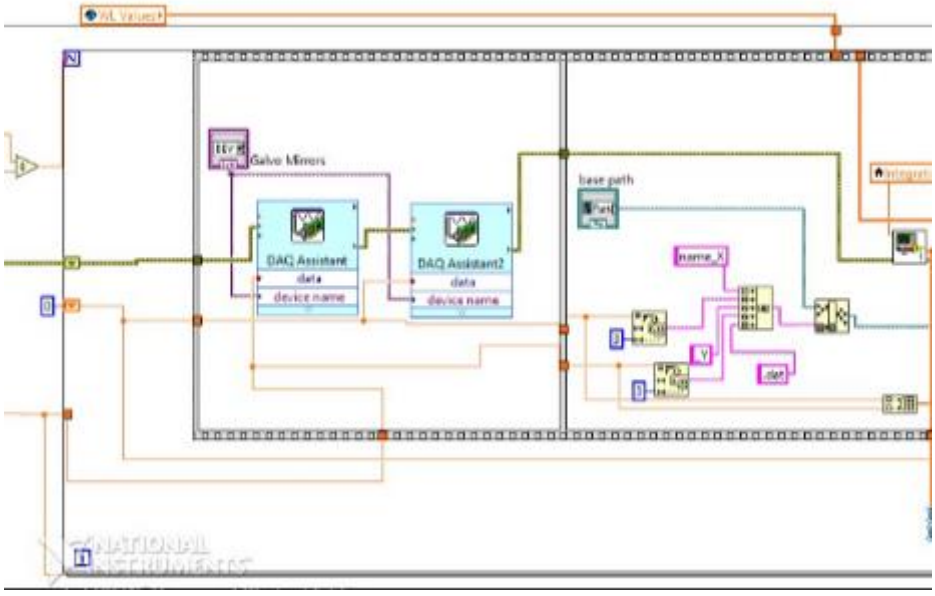

Figure 55. Terminal window of galvo_mirrors_scan LabVIEW program

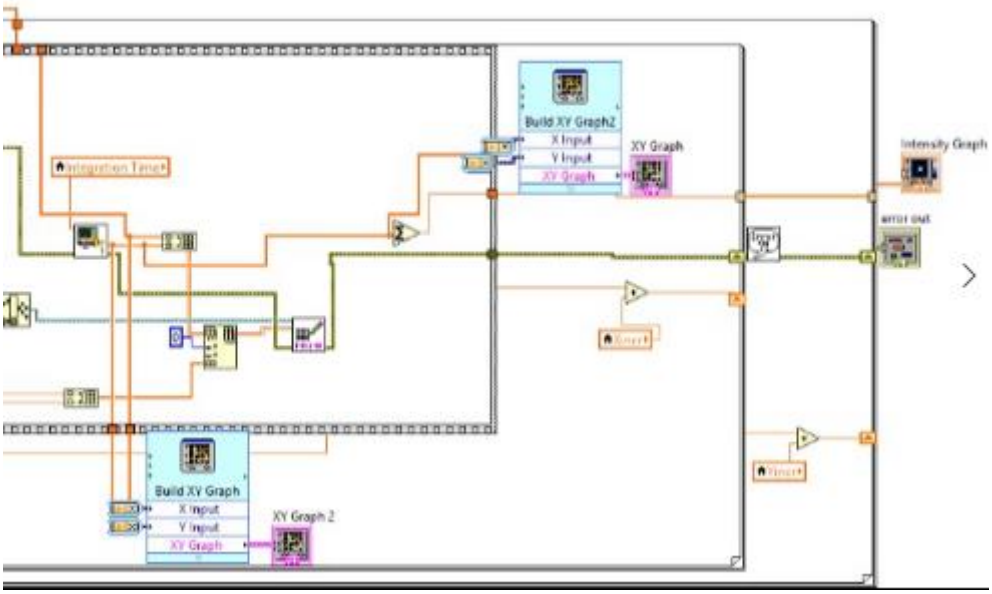

Figure 56. Terminal window of galvo_mirrors_scan LabVIEW program

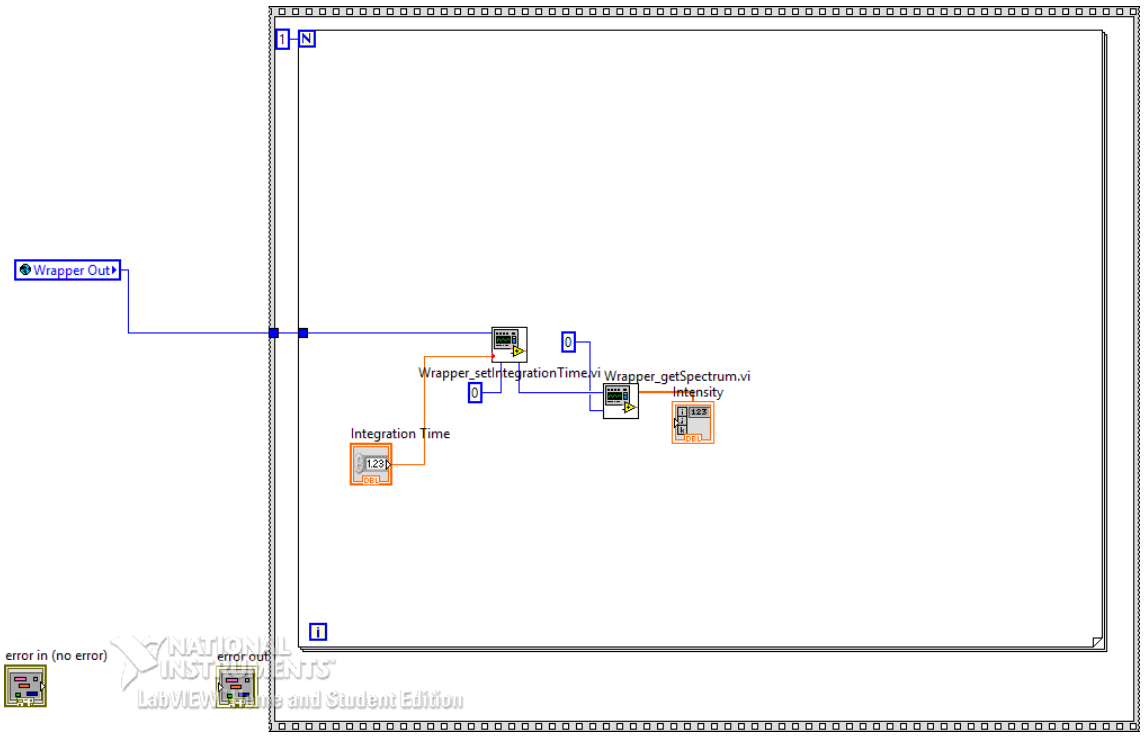

Figure 57. Terminal window of omnidriver_read LabVIEW program

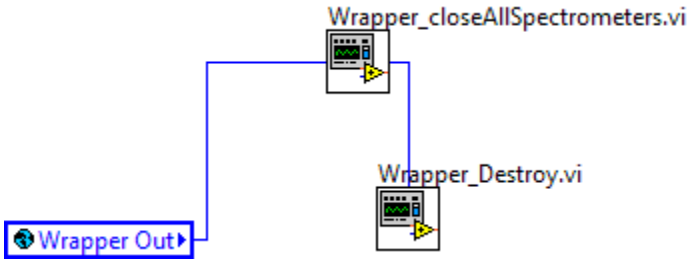

Figure 58. Terminal window of omnidriver_close LabVIEW program

Bibliography

[1] Gowen, A. A., Burger, J., O'Callaghan, D., & O'Donnell, C. P. (2009). Potential applications of hyperspectral imaging for quality control in dairy foods. In 1st international workshop on computer image analysis in agriculture, Potsdam, Germany.

[2] HELICoiD is a European collaborative project funded by the Research Executive Agency, through the Future and Emerging Technologies (FET-Open) programme, under the 7th Framework Programme of the European Union. Retrieved from http://ubimon.doc.ic.ac.uk/helicoid/m1860.html

[3] Alfano, A.A., et-al "Optical Spectroscopic Diagnosis of Cancer and Normal Breast Tissues," J. Opt. Soc. Am. B, Vol. 6, No. 5, Pp. 1015-1023, May 1989. Return to Text

[4]http://ffden2.phys.uaf.edu/webproj/212_spring_2014/Amanda_Mcpherson/Amanda_McPherson/2nd_page.html

[5] Wave. (2016, June 14). In *Wikipedia, The Free Encyclopedia*. 2016. Retrieved from https://en.wikipedia.org/w/index.php?title=Wave&oldid=725254927

[6] Sengpielaudio. (n.d.). What is Amplitude? Definition of Amplitude in the Terms of Sound. Retrieved from http://www.sengpielaudio.com/calculator-amplitude.htm

[7] Visible spectrum. (2016, May 16). In *Wikipedia, The Free Encyclopedia*. 2016, Retrieved from https://en.wikipedia.org/wiki/Visible_spectrum

[8] Electromagnetic Radiation. (n.d.). Retrieved from http://www.ces.fau.edu/nasa/module-2/radiation-sun.php

[9] Pitris, C. Light-Tissue Interaction (n.d.). Retrieved from. http://www.eng.ucy.ac.cy/cpitris/tmp/ASS2013/1.2.%20Light-Tissue%20Interaction.pdf

[10] Diffuse reflection. (2016, June 13). In *Wikipedia, The Free Encyclopedia*. 2016, Retrieved from https://en.wikipedia.org/w/index.php?title=Diffuse_reflection&oldid=725079343

[11] Lens (Optics) (2016, June 17). In *Wikipedia, The Free Encyclopedia*. 2016, Retrieved from https://en.wikipedia.org/w/index.php?title=Focal_length&oldid=722033531

[12] Nave, Carl R. "Thin Lens Equation". *Hyperphysics*. Georgia State University. RetrievedMarch 17, 2015.

[13] Crouch, Stanley; Skoog, Douglas A. (2007). *Principles of instrumental analysis*. Australia: Thomson Brooks/Cole. ISBN 0-495-01201-7.

[14] Brand, John C. D. (1995). *Lines of Light: The Sources of Dispersive Spectroscopy, 1800 - 1930*. Gordon and Breach Publishers. pp. 37–42. ISBN 2884491627.

[15] IUPAC, *Compendium of Chemical Terminology*, 2nd ed. (the "Gold Book") (1997). Online corrected version: (2006–) "resolution in optical spectroscopy".

[16] Charge-coupled device (2016, June 17). In *Wikipedia, The Free Encyclopedia*. 2016, Retrieved from https://en.wikipedia.org/wiki/Charge-coupled_device

[17] Thermal and Statistical Physics (n.d.) Retrieved from http://www.patarnott.com/phys625/notes2011_phys625.htm

[18] Multispectral vs Hyperspectral Imagery Explained. (2016). Retrieved from http://gisgeography.com/multispectral-vs-hyperspectral-imagery-explained/

[19] Akbari, H., Halig, L. V, Schuster, D. M., Osunkoya, A., Master, V., Nieh, P. T., … Fei, B. (2012). Hyperspectral imaging and quantitative analysis for prostate cancer detection. *Journal of Biomedical Optics*, *17*(7), 760051–7600510. Retrieved from http://dx.doi.org/10.1117/1.JBO.17.7.076005

[20] Instructions, O. (n.d.). and and Scanning Galvo Systems User Guide, 1–40. Retrieved from http://www.thorlabs.com/thorcat/20300/GVS012-Manual.pdf

[21] Guide, U (n.d.) NI USB-6008/6009. Bus-Powered Multifunction DAQ USB Device

[22] Jacobs, Donald H. Fundamentals of Optical Engineering. MC Graw-Hill Book Co., 1943.

[23] Spark-vis, F. P., & Ave, D. (n.d.). Spark Spectral Sensor User Manual. Retrieved from http://oceanoptics.com/wp-content/uploads/SPARKManual.pdf

[24] Optics, O. (n.d.) DH-2000 Deuterium-Halogen Light Source Installation and Operation Manual. Retrieved from http://oceanoptics.com//wp-content/uploads/DH-2000-Installation-and-Operation-Instructions.pdf

[25] LabVIEW (2016, June 9).). In *Wikipedia, The Free Encyclopedia*. 2016, Retrieved from https://en.wikipedia.org/wiki/LabVIEW